Secreted frizzled-related protein 2 (sFRP2) redirects non-canonical Wnt signaling from Fz7 to Ror2 during vertebrate gastrulation

DISSERTATION

submitted to the
Combined Faculties of the Natural Sciences and for Mathematics
of the Ruperto-Carola University of Heidelberg, Germany
for the degree of
Doctor of Natural Sciences

Eva-Maria Brinkmann
2015

Dissertation
submitted to the
Combined Faculties of the Natural Sciences and for Mathematics
of the Ruperto-Carola University of Heidelberg, Germany
for the degree of
Doctor of Natural Sciences

presented by

Dipl.-Ing./ M.Sc Eva-Maria Brinkmann
born in: Steinfurt, Germany
Oral examination: ……

Secreted frizzled-related protein 2 (sFRP2) redirects non-canonical Wnt signaling from Fz7 to Ror2 during vertebrate gastrulation

Referees:

Dr. Suat Özbek

Prof. Dr. Thomas Holstein

This thesis is dedicated to
Herbert Steinbeisser.

Acknowledgements

The past 4 years at the University of Heidelberg were very formative and full of precious experiences. I would not have made it successfully without the contribution of the following people.

My deepest appreciation goes to my supervisor Herbert Steinbeisser who gave me the opportunity to work in his research group. Herbert, thank you for your excellent guidance, encouragement and scientific feedback. You were a great mentor for me.

I am deeply grateful to Suat Özbek and Lilian Kaufmann, who supervised and supported me at the end of my thesis. Thank you for your guidance, constant interest and valuable suggestions. Without you, I wouldn´t have been able to bring my thesis to a good end.

Special thanks to Christof Niehrs and to the members of the Niehrs group for supportive discussions and progress reports.
My Thesis committee guided me through all the years. Thank you to Gary Davidson and Thomas Holstein for being my advisors and for your support.

I will forever be thankful to all the Steinbeisser lab members who have been supportive in every way. Anne, Anja, Inge, Judith, Kirsten, Maria, Nastassja, Rahul and Susanne. Thank you all for the enormous amount of support, help, all the laughter and fun. It was a wonderful time and I enjoyed working with every single person.

I especially thank my family and friends. You were always supportive and encouraged me with your best wishes.

Finally, I would like to thank my boyfriend. Words cannot express how grateful I am. Thank you, you always took so much care of me, supported me with everything, all your love and encouraged me throughout this time. We grew a lot in it!
To my beloved daughter, I would like to express many thanks for being such a good girl always cheering me up.

Table of Contents

1 Summary

Proper cell movements require balanced activities of different signaling cascades, but factors regulating this interplay on the molecular level are poorly characterized. During embryogenesis, convergent extension (CE) movements are mainly regulated by three branches of non-canonical Wnt signaling: Ror2 mediated signaling, Frizzled mediated classical Wnt/PCP signaling, and the Wnt/Ca^{2+} signaling pathway. Secreted frizzled-related proteins (sFRPs) are known as inhibitors or biphasic modulators of Wnt/β-catenin signaling but less is known about their function in β-catenin independent Wnt pathways.

Here, I show that secreted frizzled-related protein 2 (sFRP2), a member of the sFRP family, is required for morphogenesis and *papc* expression during *Xenopus* gastrulation. Notably, sFRP2 redirects non-canonical Wnt signaling from Fz7 to Ror2. During this process, sFRP2 promotes Ror2 signal transduction by stabilizing Wnt5a/Ror2 complexes at the membrane while it inhibits Fz7 signaling, probably by blocking Fz7 receptor endocytosis.

Direct interaction of the two receptors via their CRDs also promotes Ror2 mediated *papc* expression but inhibits Fz7 signaling. Furthermore, other Fz-CRD containing proteins, such as other sFRP1 and frzb2 can also mediate this function. While the cysteine-rich domain (CRD) of sFRP2 is sufficient for Ror2 activation, the NTR domain of sFRP2 seems to be important for efficient Fz7 inhibition since the CRD alone could not prevent Fz7 receptor internalization.

Based on my results, I propose that sFRPs act as a molecular switch channeling the signal input for different non-canonical Wnt pathways during vertebrate gastrulation.

Zusammenfassung

Zellbewegungen erfordern streng regulierte und aufeinander abgestimmte Signale, welche jedoch derzeit noch weitgehend ungeklärt sind. Während der Embryogenese werden konvergente Extensionsbewegungen hauptsächlich durch drei nicht kanonische Wnt- Signalwege reguliert: 1. Durch Ror2 vermittelte Signaltransduktion, 2. Durch den klassische Wnt/PCP Signalweg und 3. Durch die Wnt/Ca^{2+} Signalkaskade.

Studien haben bereits mehrfach gezeigt, dass secreted frizzled-related proteins (sFRPs) den kanonischen Wnt/β-catenin Signalweg modulieren können. Über ihre Funktionen im Bezug auf den nicht kanonischen Wnt-Signalweg ist allerdings wenig bekannt. In dieser Arbeit konnte ich zeigen, dass sFRP2, welches zu der Familie der sFRPs angehört, für die Morphogenese und die *papc*-Expression während der *Xenopus*-Gastrulation erforderlich ist. Insbesondere lenkt sFRP2 die nicht kanonische Signaltransduktion vom Fz7 zum Ror2 Rezeptor um. Dabei fördert sFRP2 einerseits die Ror2 induzierte Signalkaskade, indem es Wnt5a/Ror2-Komplexe stabilisiert. Andererseits hemmt sFRP2 dagegen Fz7-vermittelte Signale, vermutlich durch eine Inhibierung der Rezeptorendocytose.

Darüber hinaus führt eine direkte Interaktion von beiden Rezeptoren über ihre Cystein-reiche Domäne (CRD) auch zu einer erhöhten Ror2-, aber einer verminderten Fz7-Signaltransduktion. Auch andere Proteine, wie sFRP1 oder frzb2, die über solch eine CRD verfügen, können diesen Effekt vermitteln. Die CRD von sFRP2 ist ausreichend für die Ror2-Aktivierung. Jedoch scheint die NTR-Domäne, für eine effiziente Fz7 Inhibierung erforderlich zu sein, da die CRD von sFRP2 allein das Fz7-vermittelte Signal nicht hemmen kann.

Auf Grundlage meiner Ergebnisse lässt sich folgern, dass sFRPs während der Gastrulation als molekularer Schalter fungieren, die das nicht kanonische Signal von dem einen auf den anderen Rezeptor umlenken können.

2 Introduction

2.1 *Xenopus* gastrulation movements

Embryogenesis is a complex process, in which a single cell proliferates and gives rise to a multitude of highly specialized cells that finally develop into specific tissues and organs of a living organism. This is achieved by multiple signaling events, cell differentiation and concerted cell movements.

Gastrulation is defined and coordinated by four types of region specific cell movements: invagination, involution, epiboly and convergent extension (CE) movements. These cell and tissue movements thereby force an unstructured group of cells to reorganize to an embryo composed of the three germ layers: endoderm, mesoderm and ectoderm. An ideal model to study the regulation of these processes is the African clawed frog (*Xenopus laevis*). After the *Xenopus* oocyte is fertilized, the zygote is cleaved several times without increasing its cell mass. At the end of cleavage a blastula embryo is formed which consists of several thousands of undifferentiated, pluripotent cells and a liquid filled cavity, the blastocoel (Fig. 1, Blastula; stage 8)

Subsequently, gastrulation starts on the future dorsal side of the embryo. During this process, specific growth factors induce the formation of so called bottle cells from a group of endodermal cells by apical constriction. These cells migrate into the embryo and thereby form the invagination (blastopore) (Fig. 1, Early gastrula; stage 10) (Keller, 1981; Lee and Harland, 2010). This is followed by involution of mesodermal cells, which migrate towards the animal cap (Fig. 1, Gastrula; stage 11) by convergent extension (CE) movements to establish the anterior-posterior (AP) axis (see 2.1.1). Meanwhile, the cells of the animal cap move downwards to the vegetal pole by epiboly. During epiboly the cells intercalate and stretch and by the end of gastrulation, ectodermal cells cover the entire embryo (Fig. 1, Late Gastrula; stage 12) (Keller, 1980). Mesendodermal and ectodermal cell populations do not fuse and a morphologically visible tissue border, the Brachet´s cleft arises.

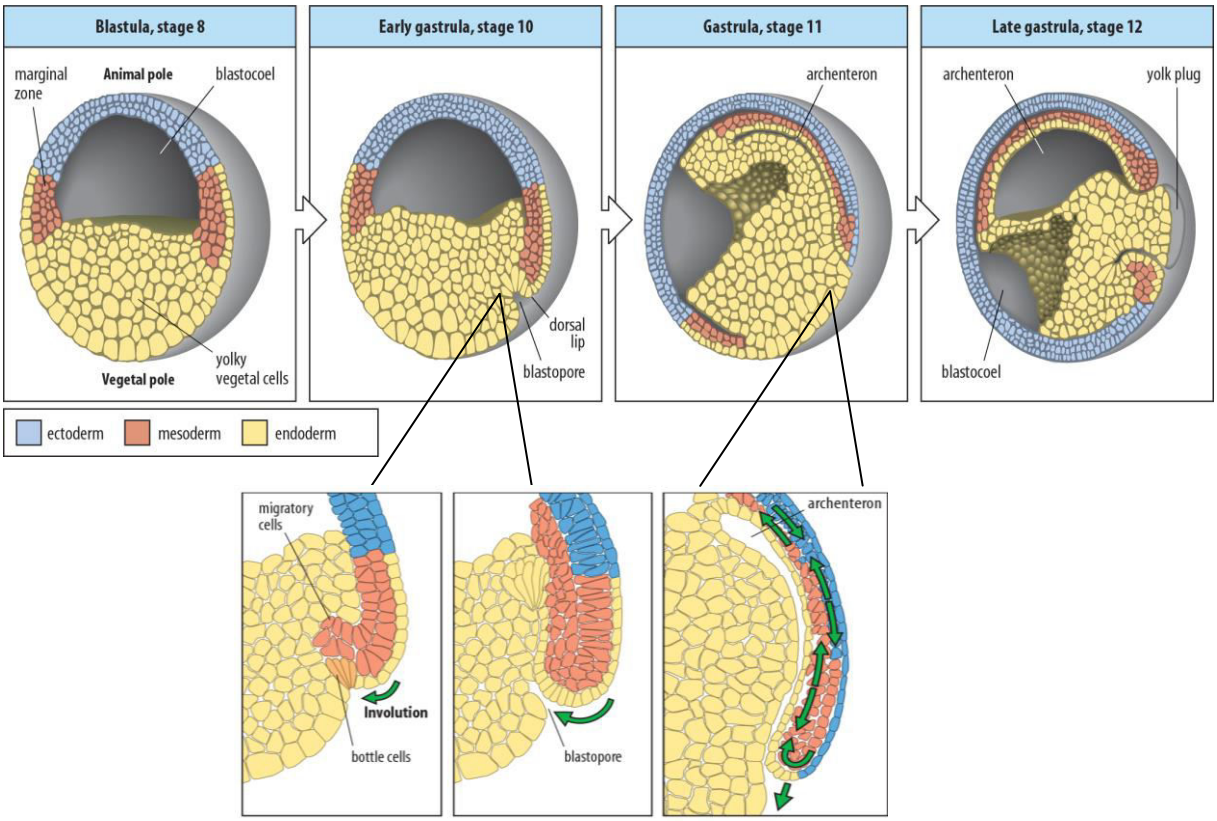

Fig. 1: **Schematic drawing of early *Xenopus* gastrulation.** At late blastula (stage 8) the animal cap region consists of the prospective ectoderm. The future mesoderm and endoderm are located in the marginal zone. In early gastrula (stage 10) the formation of bottle cells via apical constriction is induced on the dorsal side of the embryo. This leads to the formation of the blastopore. C: During midgastrula (stage11) mesoderm cells involute through this blastopore and move in close contact along the ectoderm cells towards the anterior. A border, *Brachet's* cleft, persist between the involuted mesoderm and the ectoderm. At late gastrula (stage 12), the yolk plug is visible through the blastopore and animal cap cells cover the entire embryo (adapted and modified from Wolpert; Principles of Development).

2.1.1 CE movements establish the anterior-posterior (AP) axis

Convergent extension (CE) is an important process during development to achieve a change in tissue shape.

The best-studied example of CE is the elongation of the axis during *Xenopus* gastrulation. Moreover, also in other vertebrate and invertebrate systems, CE represents a common process that mediates body axis elongation (Glickman et al., 2003; Munro and Odell, 2002; Sausedo and Schoenwolf, 1994; Schoenwolf and Alvarez, 1989).

When mesodermal cells migrate through the blastopore by CE movements they acquire a bipolar shape and due to their protrusive activity on the neighbouring cells

they pull themselves between each other. During this process, the tissue simultaneously narrows (convergence) in mediolateral direction and lengthens (extension) in perpendicular direction (Keller et al., 1985). The combination of collective cell movement and cell intercalation thereby establishes the AP axis of the embryo (Fig. 2).

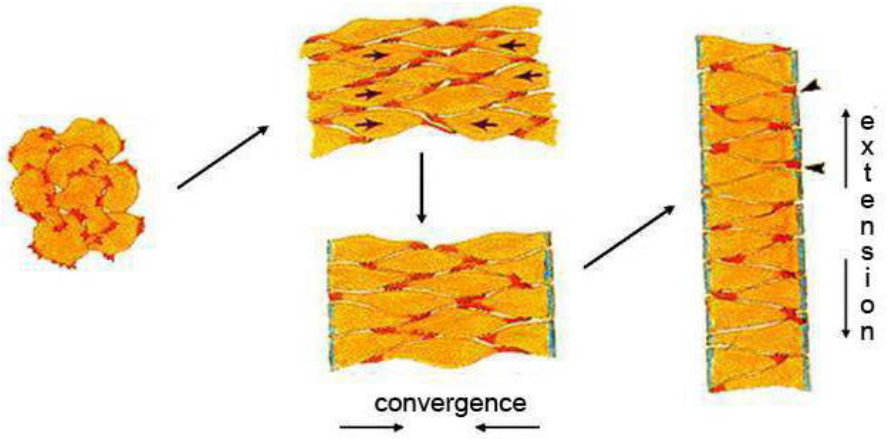

Fig. 2: **Convergence and extension:** Involuting mesodermal cells undergo convergent extension movements in which multipolar cells acquire a bipolar shape and converge at the dorsal midline. By cell intercalations the tissue narrows and elongates (adapted from (Keller, 2002)).

2.2 Gastrulation and CE movements are regulated by the Wnt signaling network

A tight regulation and a fine-tuned crosstalk of different signaling pathways are required for proper cell movements during *Xenopus* gastrulation.

Several studies demonstrate that the ß-catenin independent (non-canonical) Wnt/Planar Cell polarity (PCP), Wnt5a/Ror2 and Wnt/Ca^{2+} pathways are important regulators for CE movements (Schambony and Wedlich, 2007; Seitz et al., 2014; Torres et al., 1996; Veeman et al., 2003; Wallingford et al., 2002). However, also the Wnt/ß-catenin dependent (canonical) pathway (Kuhl et al., 2001) and BMP signaling have been implicated in morphogenesis (Myers et al., 2002).

Wnt signaling is mediated by Wnt proteins that bind to the extracellular cysteine rich domain (CRD) of seven-transmembrane receptors of the Frizzled (Fz) family. 10 different Fz receptors exist in human as well as 19 genes that encode Wnt proteins. Fz receptors act as a common receptor for both canonical (β-catenin dependent) or

non-canonical (β-catenin independent) Wnt signaling and depending on the cellular context, a co-receptor or Wnt ligand of one of these cascades is activated (Niehrs, 2012). However, it is still controversial which co-receptors and downstream effectors they are coupled to and moreover to what extend these pathways overlap.

2.2.1 The Canonical Wnt/ß-catenin pathway

The canonical Wnt/ β-catenin cascade is the best characterized branch of the Wnt signaling network and plays a critical role in early embryonic pattering, stem cell renewal and cancer (Komiya and Habas, 2008). In many organisms, this signaling pathway directs axis formation. For example in In *Xenopus*, loss of maternally provided β-catenin results in ventralized embryos. Furthermore, over stimulation of canonical Wnt signaling at the ventral side of a *Xenopus* embryo leads to the formation of double axis (McCrea et al., 1993). A hallmark of this pathway is the core protein β-catenin and whose cellular level is controlled by a destruction complex. In the absence of a Wnt ligand, the destruction complex machinery composed of adenomatous polyposis coli (APC), Axin, Casein Kinase 1 (CK1) and Glycogen Synthase Kinase 3 (GSK3) is located in the cytosol and marks β-catenin molecules by phosphorylation for subsequent ubiquitination and proteosomal degradation. (Niehrs, 2012) (Fig. 3: Unstimulated).

Canonical Wnt signaling is activated when Wnt binds to a receptor complex composed of Fz and the co-receptors low-density lipoprotein receptor-related protein 5/6 (LRP5/6) forming a dimeric/multimeric structure. This triggers phosphorylation of LRP5/6 by CK1 and GSK3-β which in turn leads to association of GSK3 with the scaffold protein Axin. Meanwhile, Fz interacts with Dishevelled (Dvl) (Chen et al., 2003; Tauriello et al., 2012), which in turn promotes interaction with Axin (Fiedler et al., 2011; Schwarz-Romond et al., 2007). These events disrupt the APC/Axin/CK1/GSK3 machinery and therefore phosphorylation of β-catenin by CK1 and GSK3. β-catenin accumulates in the cytoplasm and is subsequently translocated into the nucleus where it associates with transcription factors such as TCF (T cell factor) and LEF (lymphoid enhancer-binding factor) to mediate transcriptional induction of target genes (Fig. 3: Stimulated).

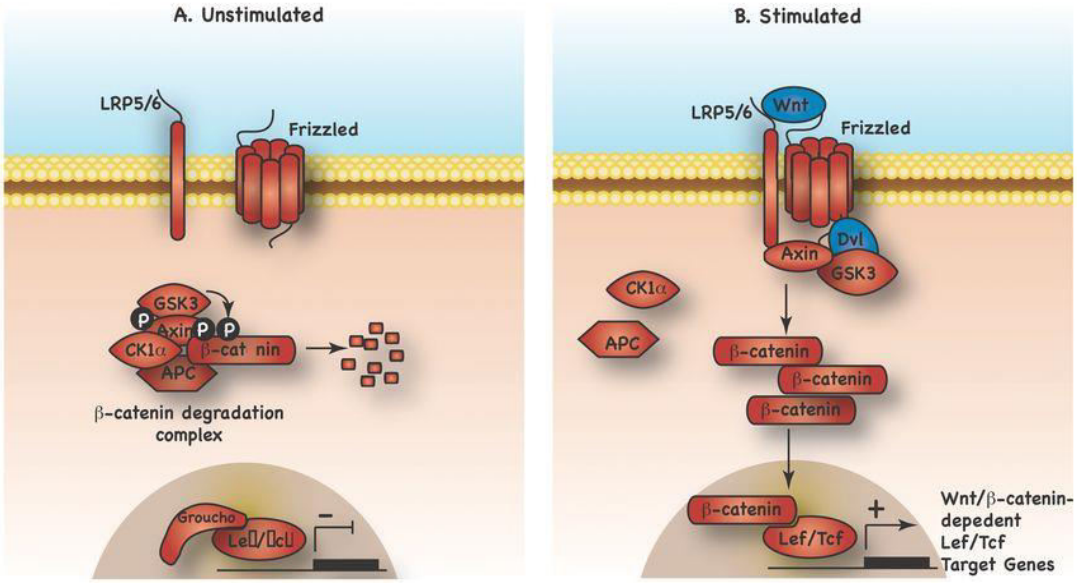

Fig. 3: Overview of the canonical Wnt/β-catenin pathway. A: In the absence of a Wnt ligand β-catenin is marked for proteosomal degradation by the destruction complex **. B:** Wnt ligand binding inhibits the destruction complex and thereby leads to accumulation of β-catenin in the nucleus and activation of Wnt target genes. Adapted from **http://d2q6k56aomjvqy.cloudfront.net/content/ppbiochemj/427/1/1/F1.large.jpg**.

2.2.2 Non-canonical Wnt signaling pathways

In contrast to the canonical Wnt pathway, several pathways exists that do not involve the function of β-catenin. These pathways are often summarized as “non-canonical” Wnt pathways. The output of these non-canonical cascades mostly regulates cytoskeletal rearrangements and cell migration and has less effect on cell differentiation and proliferation (Niehrs, 2012). However there are several distinct β-catenin independent pathways known to date. The three most important pathways for gastrulation movements are described in the following sections.

2.2.2.1 Wnt/PCP signaling

The term “planar cell polarity” (PCP) is derived from a study of tissue polarity necessary to generate polarization within the plane of the epithelium in Drosophila (Nubler-Jung et al., 1987). Also, in vertebrates PCP was shown to be involved in cellular processes such as the orientation of stereocilia in the inner ear (Kikuchi et al., 2011; Simons and Mlodzik, 2008), ordered arrangement of hairs of mammalian skin

and cilia of respiratory tract, or orientation of axon extension (Goodrich, 2008). In *Xenopus*, the Wnt/PCP pathway is a key regulator of cell movements during gastrulation, in particular CE movements, which requires the polarisation of the cells to enable their mediolateral intercalation and the elongation along the perpendicular AP axis (Wang and Steinbeisser, 2009). Numerous studies showed that inactivation as well as stimulation of this pathway leads to gastrulation defects such as a shorter AP axis or *spina bifida* (Djiane et al., 2000; Sumanas and Ekker, 2001).

Wnt/PCP signaling does not involve stabilization of β-catenin and LEF/TCF mediated transcription in the nucleus. This signaling cascade is thought to be independent from the co-receptors LRP5 and LRP6 but is characterized by membrane recruitment of Dishevelled (Dvl) after Wnt stimulation (Axelrod et al., 1998). This pathway further involves the small GTPases RhoA, Rock and c-jun-N-terminal kinase (JNK) which are important regulators for cytoskeleton and actin polymerization. Ultimately, JNK dependent transcription factors, for example activating transcription factor 2 (ATF2) and activator protein 1 (AP-1), are activated (Fig. 4). While in Drosophila it is still unclear whether a Wnt ligand is involved in the PCP pathway, it has been shown in vertebrates that Wnt5a and Wnt11 can trigger this cascade. Wnt/PCP signal transduction was further suggested to require clathrin-mediated Fz receptor endocytosis. It was shown that direct interaction of Dvl2 with the clathrin AP-2 adaptor, an effector of endocytic traffic from the plasma membrane to endosomes, was essential to transduce Wnt/PCP signaling (Kim et al., 2008; Yu et al., 2010). However, the molecular mechanism regulating the process of Wnt/Fz endocytosis and downstream signaling is not fully understood.

2.2.2.2 Wnt/Ca^{2+} pathway

Wnt/Fz binding also triggers a second branch of the non-canonical Wnt pathway termed as the Wnt/Ca^{2+} pathway. It shares some components with the PCP pathway including Dvl, the Wnt ligand and Fz receptor but involves mobilization of intracellular Ca^{2+} from the endoplasmatic reticulum (ER) and activation of Ca^{2+} sensitive proteins such as Protein Kinase C (PKC) and calcium/calmodulin-dependent kinase II (CamKII). This pathway further depends on the function of heterotrimeric G-proteins. These proteins activate phospholipase C (PLC) which is turn cleaves phospholipid phosphatidylinositol 4,5 bisphophat (PIP2) into diacylglycerol (DAG) and

inositol-1,4,5-trisphosphate (IP3). IP3 diffuses through the cytosol where it binds to calcium channels on the ER membrane to mediate intracellular release of Ca^{2+} molecules. The accumulation of Ca^{2+} in the cytoplasm further stimulates Ca^{2+} sensitive proteins such as PKCα and CamKII (Fig. 4).

Increased Ca^{2+} also stimulates calcineurin and CamKII which in turn activate the cytoplasmic protein nuclear factor associated with T-cells (NFAT) to regulate cell adhesion, migration and tissue separation. In addition, CamKII also activates Nemo Like kinase (NLK) which interferes with TCF/β-catenin signaling in the canonical Wnt pathway (Komiya and Habas, 2008).

In humans, fiftheen PKC isoforms exists and depending on the messenger they require to be activated they are divided into the following subfamilies: classical (conventional) (cPKC), novel (nPKC) and atypical (aPKC). cPKC family members contain the isoforms α, βI, βII, γ and are mainly activated by Ca^{2+} and DAG. The nPKC subgroup includes the isoforms δ, ε, θ and η, which are not activated by Ca^{2+} but through DAG. Members of the aPKC subgroup cannot be stimulated by either of these two molecules (Mellor and Parker, 1998).

In *Xenopus* over-expression of Wnt5a or Wnt11 ligands can activate PKCα (Sheldahl et al., 1999) and calcium/calmodulin-dependent kinase II (CamKII) (Kuhl et al., 2000a; Kuhl et al., 2000b). This signaling branch is suggested to control the regulation of cell sorting behaviour. Loss of zygotic Fz7 leads to the inability of involuted mesoderm to separate from the ectoderm but is rescued by co-expression of PKCα. Furthermore, they showed that Fz7 induces activation and recruitment of PKCα to the cell membrane in the context of tissue separation during *Xenopus* gastrulation (Winklbauer et al., 2001).

2.2.2.3 Wnt5a/Ror2 pathway

Fz receptors and LRP5/6 were the first proteins implicated as receptors for Wnt ligands, but they are by far not the only ones (Clevers and Nusse, 2012). The receptor tyrosine kinase-like orphan receptors Ror1 and Ror2 are members of the receptor tyrosine kinases (RTKs) and identified in PCR based screens for proteins with resemblance to tyrosine kinases of the Trk family (Masiakowski and Carroll, 1992). They contain a CRD homologous to the Wnt-binding domain found in Fz receptors (Saldanha et al., 1998). In addition to the CRD, they are further

characterized by an extracellular Kringle, immunoglobulin and intracellular proline-rich and serine-threonine-rich domains (Masiakowski and Carroll, 1992). Ror1 and Ror2 are single-pass transmembrane proteins and evolutionarily conserved across vertebrate and invertebrate species. Studies have shown that forced dimerization induces Ror2 tyrosine phosphorylation, whereas ligand binding can induce either tyrosine or serine/threonine phosphorylation (Akbarzadeh et al., 2008; Grumolato et al., 2010; Liu et al., 2007; Liu et al., 2008; Mikels et al., 2009; Yamamoto et al., 2007). Recently, it was shown that Ror2 interacts with Wnt5a to induce the expression of paraxial protocadherin (*papc*) and involved in the regulation of CE movements (Djiane et al., 2000; Hikasa et al., 2002; Schambony and Wedlich, 2007). The Wnt5a/Ror2 pathway has been suggested to form an additional branch of the β-catenin independent signaling network, likely requiring phosphoinositide 3 kinase (PI3K), CDC42, and MKK7 to activate JNK signaling (Fig. 4), rather than RhoA and Rac1, which are activated by Fz7 (Schambony and Wedlich, 2007). In humans, Brachydactyly type B and recessive Robinow syndrome, which result in limb malformations are associated with mutation in Ror2 (Afzal and Jeffery, 2003; Afzal et al., 2000; Oldridge et al., 2000). Furthermore, a recent study presents Ror2 as a novel prognostic biomarker and potential therapeutic target in patients with leiomyosarcomas or gastrointestinal stromal tumors (Edris et al., 2012).

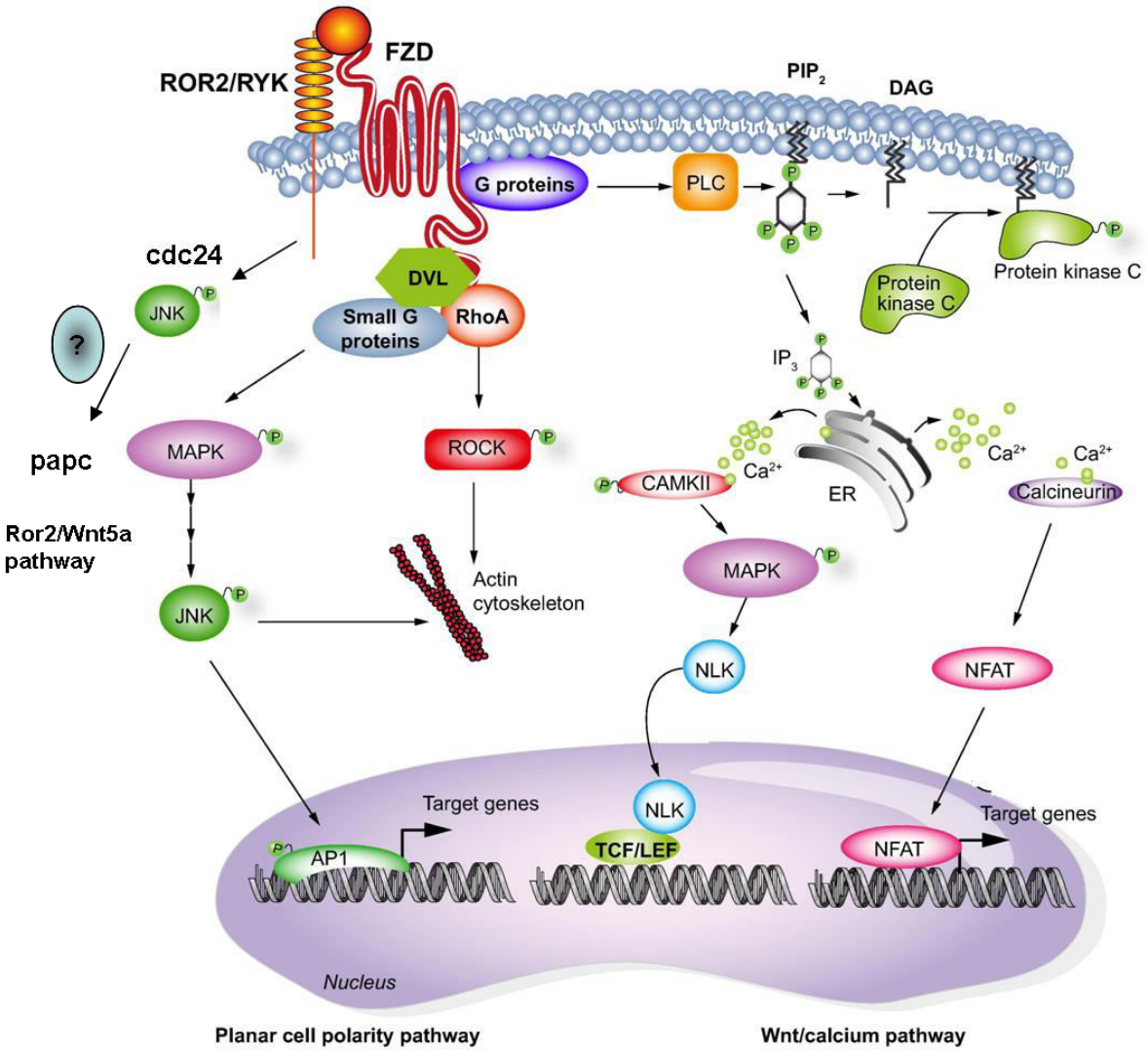

Fig. 4: Overview of the β-catenin independent Wnt signaling branches: Ror2/Wnt5a signaling (left cascade), Frizzled mediated Planar Cell polarity (middle cascade) and Wnt/Calcium signaling (right cascade). Modified from: **http://pharmaceuticalintelligence.com/2015/04/10/targeting-the-wnt-pathway-7-11/.**

2.3 Secreted modulators of Wnt signaling

Wnt signaling can be regulated by a wide range of effectors which can either interfere with the intracellular components of the signaling cascade or modulate ligand-receptor interactions in the extracellular space. Effectors can function as agonists to enhance a signaling event or as antagonists to inhibit a response. They are of great importance as they control and fine tune Wnt signaling and thereby play a crucial role in development and disease (Cruciat and Niehrs, 2013).There are different types of secreted Wnt modulators. Within this work, I especially focus on secreted Frizzled-related proteins (sFRPs) and the family of Dickkopf (Dkk) proteins described in the

following sections. However, Wnt signaling can be further controlled by different other antagonists such as wnt inhibitory factor 1 (WIF1), Cerberus and Sclerostin (Cruciat and Niehrs, 2013).

2.3.1 Secreted Frizzled-Related Protein (sFRP) Family

sFRPs are soluble glycoproteins and represent the largest family of secreted Wnt modulators that bind to Wnt ligands and Fz receptors. They are approximately 300 amino acids in length and contain an N-terminal cysteine rich domain (CRD) and a C-terminal netrin-like (NTR) domain. The CRD of sFRPs contain 10 conserved cysteine residues and shows 30-50% sequence similarities with the Fz CRDs (Bovolenta et al., 2008). The NTR motif contains segments of positively charged residues that were shown to confer heparin-binding properties (Uren et al., 2000) and interfere with heparan proteoglycans at the cell membrane (Finch et al., 1997). This domain is also present in some other unrelated proteins, including tissue inhibitors of metallo-proteinases (TIMPs), the axon guiding protein netrin 1, type-1 procollagen C-proteinase enhancer proteins (PCOLCEs) as well as complement proteins (Banyai and Patthy, 1999). In humans, five sFRP family members, sFRP1-5, have been identified. Phylogenetic sequence analysis revealed that sFRPs can be separated into two different subgroups in which sFRP1, sFRP2 and sFRP5 cluster together in one and sFRP3 and sFRP4 in another subgroup (Fig. 5). An additional subgroup of sFRPs (Crescent, Sizzled, Sizzled-2 and Frzb-2) exists in *Xenopus*, chick and zebrafish but not in mammals (Cruciat and Niehrs, 2013). sFRPs are well known inhibitors for canonical Wnt/β-catenin (Kawano and Kypta, 2003; Wawrzak et al., 2007) and non-canonical Wnt/PCP signaling (Satoh et al., 2006; Satoh et al., 2008; Shibata et al., 2005). sFRP5 as well as sFRP2 can directly disrupt Wnt/PCP signaling. Depletion of sFRP5 increased JNK/AP1 activity in the foregut in *Xenopus* and sFRP2 inferred with PCP in eye lens fiber cells in rat and mice (Li et al., 2008; Sugiyama et al., 2010). However, subsequent observations present evidence that they also positively modulate Wnt signaling (Gorny et al., 2013; Mii and Taira, 2009; Skah et al., 2015). Genetic analyses have shown that sFRPs are involved in the regulation of AP axis elongation and somitogenesis during embryonic mouse development (Satoh et al., 2006; Satoh et al., 2008). Also, in *Xenopus* the member of the sFRP family Crescent impairs CE movements (Pera and De Robertis, 2000;

Shibata et al., 2005). They are implicated in several diseases such as cancer (Rubin et al., 2006; To et al., 2001; Turashvili et al., 2006; Zi et al., 2005) as well as pathological events including lung fibrosis (De Langhe et al., 2014), heterotopic ossification and osteolysis (Gordon et al., 2007).

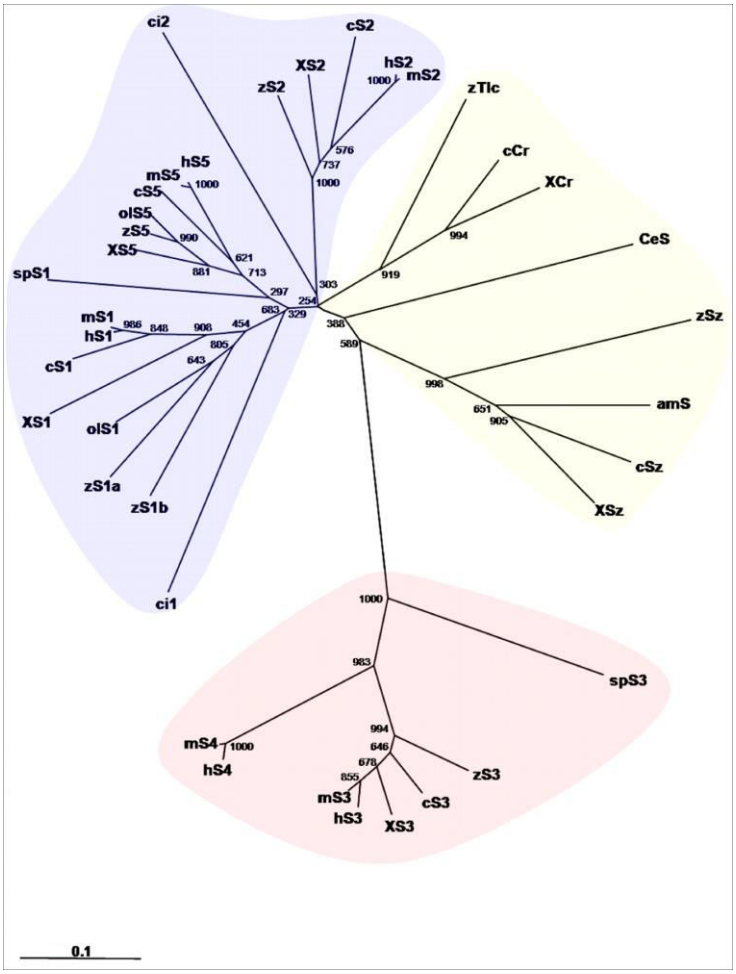

Fig. 5: Phylogentic analysis of the sFRP family obtained by homology of the CRD motif: Those displaying most similarities in amino acid sequences cluster together. The branch length is proportional to divergence and numbers indicate the bootstrap confidence for each node. Each family is represented in another colour. Am, *Ambystoma mexicanum* (axolotl); c, *Gallus gallus* (chick); Ce, *Caenorhabditis elegans* (nematode); ci, Ciona intestinalis (sea squirt); Cr, Crescent; h, *Homo sapiens* (human); m, Mus musculus (mouse); ol, Oryzias latipes (medaka fish); S, Sfrp; sp, *Strongylocentrotus purpuratus* (sea urchin); Sz, Sizzled; X, *Xenopus laevis* (African clawed frog); z, *Danio rerio* (zebrafish) adapted from (Bovolenta et al., 2008).

2.3.2 Dkk Protein Family

Dkks represent a small family of secreted proteins that comprises four members, Dkk1-4. They consist of 255-350 amino acids and have an N- terminal cysteine rich DKK_N motif unique for Dkks, as well as a C-terminal CRD, homologous to the colipase fold, but not to Fz CRDs. The colipase fold domain is present in several other unrelated proteins such as colipases, toxins or protease inhibitors (Niehrs, 2006). While Dkk1, -2 and -4 are more related to each other and are located on the same chromosome 4/5/8/10 paralogy group, Dkk3 is not part of this group and less related to those. In contrast to Dkk1, -2 and 4, Dkk 3 shares sequence similarities to soggy (sgy), also referred as to Dickkopf-like protein 1. Dkk1, -2 and 4 specifically inhibit the Wnt/β-catenin pathway by binding to LRP5 and 6. Dkk3 was rather shown to affect transforming growth factor-b (TGF-b) in *Xenopus* (Fujii et al., 2014; Mao and Niehrs, 2003; Pinho and Niehrs, 2007). Similar to sFRPs, Dkk family members are implicated in human disease, in particular cancer (Aguilera et al., 2006; Gonzalez-Sancho et al., 2005), but also in neurodegenerative processes, as well as induction of apoptosis after neuronal injury (Cappuccio et al., 2005; Caricasole et al., 2004).

Aim of this study

sFRPs are well known inhibitors of Wnt signaling and most studies have focused on their role in canonical Wnt/β-catenin signaling. Recent studies demonstrate that they also modulate non-canonical (β-catenin-independent) Wnt signaling. However, the molecular mechanism how these secreted proteins interfere with the different non-canonical Wnt signaling branches is still unknown. Therefore, this study aims to:

- Examine the effect of sFRP2 on the different non-canonical Wnt signaling branches.
- Explore the mechanism how sFRP2 exerts its activating or inhibiting function, particularly focusing on Ror2 and Fz7 mediated non-canonical Wnt signaling during vertebrate gastrulation

3 Results

3.1 Gain and Loss of sFRP2 impairs CE movements in *Xenopus*

To elucidate the role of sFRP2 during embryonic development, I performed gain and loss of function studies in *Xenopus* laevis embryos. Since sFRP2 is expressed in the dorsal mesoderm (Pera and De Robertis, 2000) and its expression pattern overlaps with known PCP pathway components such as Wnt11/5a (Shibata et al., 2005), Fz7/8 (Itoh et al., 1998; Medina et al., 2000) and Ror2 (Hikasa et al., 2002), I suspected a role for sFRP2 in the Wnt/PCP pathway. This pathway is a major regulator of CE movements and inactivation as well as stimulation leads to gastrulation defects such as a shorter AP axis or *spina bifida* (Djiane et al., 2000; Sumanas and Ekker, 2001)

I injected *Xenopus laevis sfrp2* mRNA as well as a translation blocking *sfrp2* antisense morpholino oligonucleotide (sFRP2 Mo) into the dorsal marginal zone of 4-cell stage *Xenopus* embryos and observed that both over-expression as well as loss of sFRP2 caused typical gastrulation defects (Fig. 6). Almost all sFRP2 overexpressing embryos showed either a shorter body axis (51%) or spina bifida (45%). These result provide evidence that sFRP2 modulates non-canonical Wnt signaling. Similar to *sfrp2* from *Xenopus*, also the human homolog (*hsfrp2)* induced gastrulation defects suggesting an evolutionary conserved function. Furthermore, similar phenotypes were also observed in sFRP2 morphants (Fig. 6). Co-injection of the morpholino and human *sfrp2* (*hsfrp2*) mRNA partially rescued the loss of function phenotype, indicating that well-balanced levels of sFRP2 are required for proper gastrulation. I also characterized the effect of single domains of sFRP2 on CE movements and over-expressed sFRP2 deletion mutants that either lack the CRD (sFRP2-NTR) or the NTR domain (sFRP2-CRD) in *Xenopus* embryos. The NTR as well the CRD deletion mutant induced similar morphogenic defects as the full-length sFRP2, implicating that both domains interfere with non-canonical Wnt signaling (data not shown).

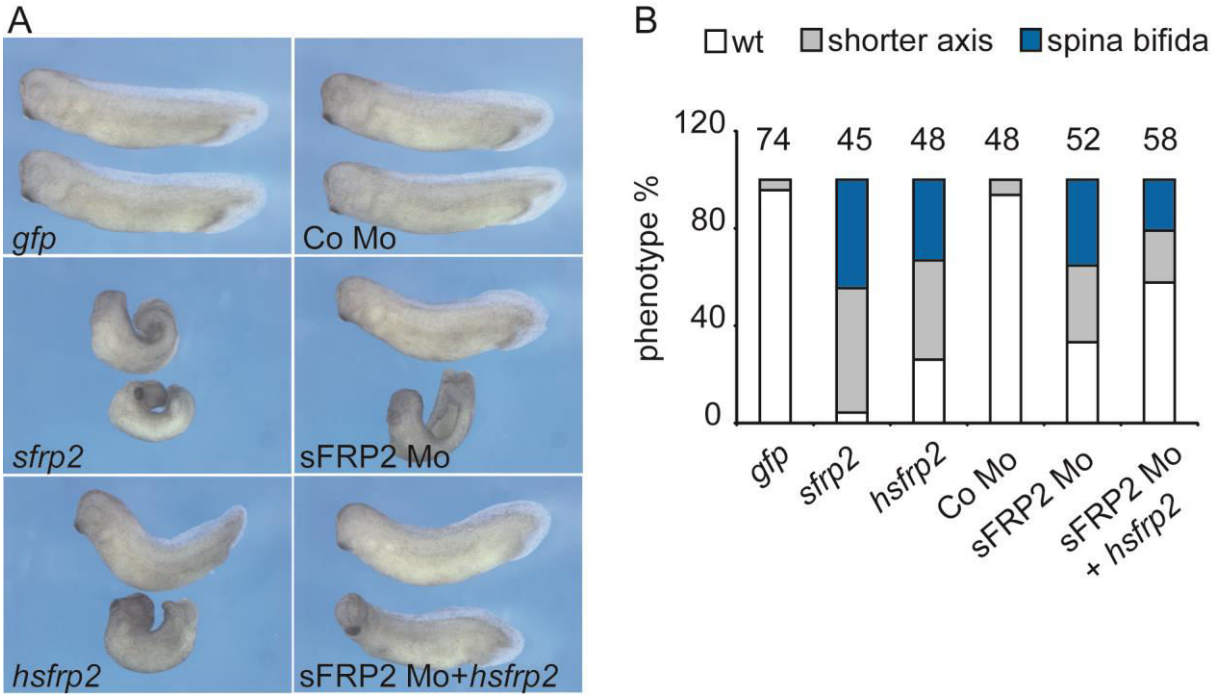

Fig. 6: **Gain and loss of sFRP2 impair CE movements in *Xenopus*. A:** Representative phenotypes of embryos injected into the dorsal equatorial zone at 4-cell stage with indicated morpholino oligonucleotides (Mo, 15ng) and synthetic mRNA (500pg *sfrp2/hsfrp2* or 200pg for the Mo-rescue). **B:** Quantification of phenotypic analysis, shown in A. Numbers of analyzed embryos are indicated on top of the bars.

To support the finding that sFRP2 affects CE movements during *Xenopus* gastrulation, I performed an elongation assay using Activin treated animal cap (AC) explants. During blastula stage, the AC region of a *Xenopus* embryo is pluripotent and can differentiate into certain types of tissues, depending on signals received from the vegetal part of the embryo. It was shown that Activin, a member of the TGF-β superfamily and FGF related growth factors, is sufficient to induce mesoderm differentiation of ectodermal explants (Brieher and Gumbiner, 1994). To test whether sFRP2 inhibits the elongation of Activin treated caps, *sfrp2* mRNA was injected in the animal region of a 2-cell stage embryo. Ror2 served as a positive control and, consistent with published data, inhibited the elongation of AC explants (Hikasa et al., 2002). In line my previous finding, showing that sFRP2 affects morphogenesis, sFRP2 also efficiently blocked the Activin induced AC elongation (Fig. 7A+B).

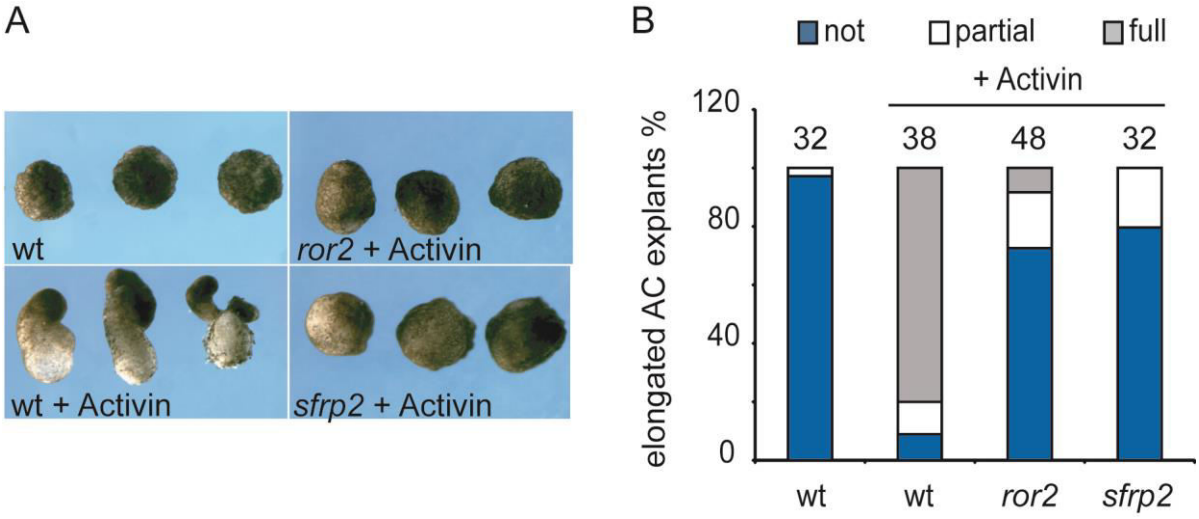

Fig. 7: **sFRP2 and Ror2 impair Activin treated animal cap elongation.** sFRP2 inhibits elongation of AC explants. **A:** For the AC elongation assay, embryos were injected animally at 2-cell stage with indicated synthetic mRNAs (300pg) and at stage 9 excised ACs were cultured with or without activin overnight to analyze elongation. **B:** Quantification of AC elongation shown in A. Categorized in not elongated (blue), partially elongated (white) and fully elongated (grey) ACs. Numbers of analyzed ACs are indicated on top of the bars.

To exclude that sFRP2 blocks AC elongation by inhibiting Activin induced mesoderm formation, I analyzed the expression of *Xbra. Xbra* is strongly up-regulated in the ring of the involuting mesoderm during *Xenopus* gastrulation and serves as a mesodermal marker (Isaacs et al., 1994). Since neither Ror2 nor sFRP2 over-expression affected the induction of the mesodermal marker gene *Xbra*, the inhibition of elongation was specifically caused by disturbed cell movements, probably due to disturbed non-canonical Wnt signaling, and not by interference with mesoderm induction (Fig.8).

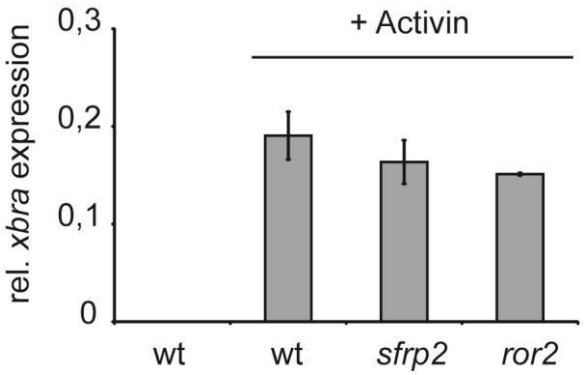

Fig. 8: **sFRP2 and Ror2 do not affect mesoderm induction.** Analysis of *xbra* expression of 10 ACs per sample, harvested after two hours incubation in Activin. Representative with technical triplicates

confirmed by at least 2 independent experiments with similar results is shown using sibling animal caps of those shown in Fig.7**.**

3.2 sFRP2 is required for *papc* expression and enhances Ror2 mediated signaling

Since previous results show that sFRP2 affects cell movements, I next investigated its effect on the pathways known to control CE movements. I focused first on Wnt5a/Ror2 signaling and analyzed the effect of sFRP2 on the activation of Wnt5a/Ror2 mediated *papc* induction (Schambony and Wedlich, 2007).

For this purpose, sFRP2 Mo was injected into the dorsal equatorial region of 4-cell stage embryos and the expression pattern of *papc* was evaluated at gastrula stage using whole mount *in situ* hybridization (Fig. 9). I observed that compared to control morpholino injected embryos, sFRP2 deficient embryos had reduced *papc* expression at the dorsal lip. This effect was similar to the *papc* pattern in Ror2 deficient embryos (Fig. 9A). Loss of Ror2 reduced the *papc* level in 61±8% of the embryos and loss of sFRP2 in 39±2% of the embryos (Fig. 9B). Consistently, sFRP2 over-expression led to increased *papc* expression compared to *gfp* control injected embryos (data not shown).

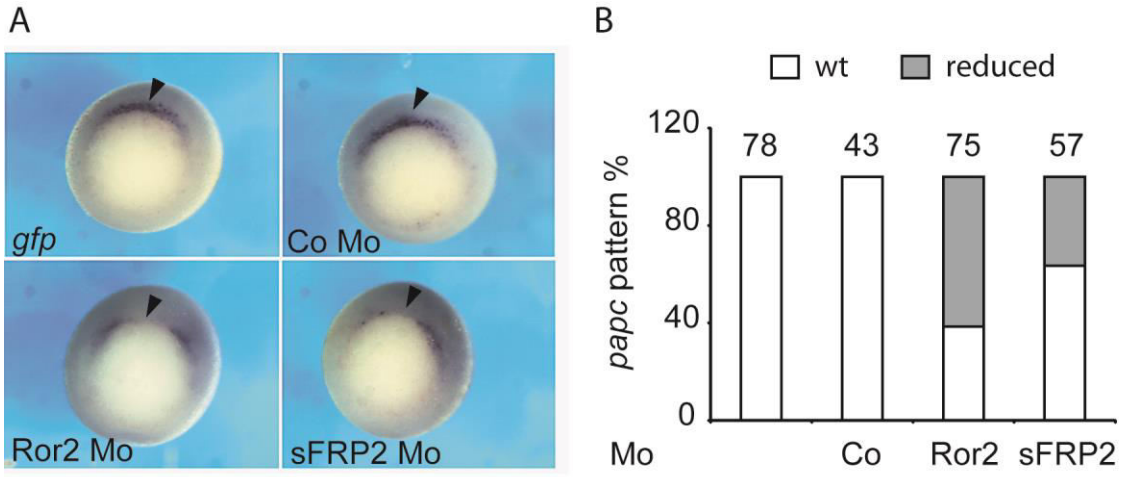

Fig. 9: **Loss of sFRP2 reduces the expression of *papc* in the dorsal lip. A:** Representative *papc* expression pattern analyzed by whole mount *in situ* hybridization of gastrula (stage10.5) embryos injected at 4-cell stage in the dorsal equatorial region with indicated Mos (15ng). Arrowheads indicate site of injection. **B:** Quantification of *in situ* hybridization, shown in A. Number of analyzed embryos indicated on top of the bars.

To verify this observation, *papc* expression was further analyzed using quantitative real time PCR (qPCR). Concurrently, loss of sFRP2 mimicked the loss of Ror2 and resulted in a significant decrease of *papc* transcription in whole embryos (Fig. 10).

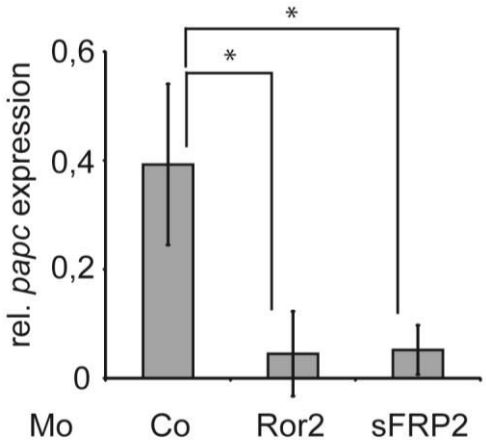

Fig. 10: **Loss of sFRP2 reduces the expression of *papc* during *Xenopus* gastrulation, similar to loss of Ror2.** Relative expression of *papc* analyzed by qPCR in whole embryos injected with indicated Mos (15 ng). Chart shows the mean ± SD of n=3 independent experiments. (*) indicates significance (*p< 0.05) compared to controls.

The reduced induction of *papc* in sFRP2 morphants could be rescued by co-injection of *hsfrp2* mRNA indicating that the sFRP2 morpholino is specific. Furthermore, the injection of *hsfrp2* mRNA induced an up-regulation of *papc* by itself (Fig. 11). Collectively, these findings show that sFRP2 is required for *papc* induction in *Xenopus* gastrulae.

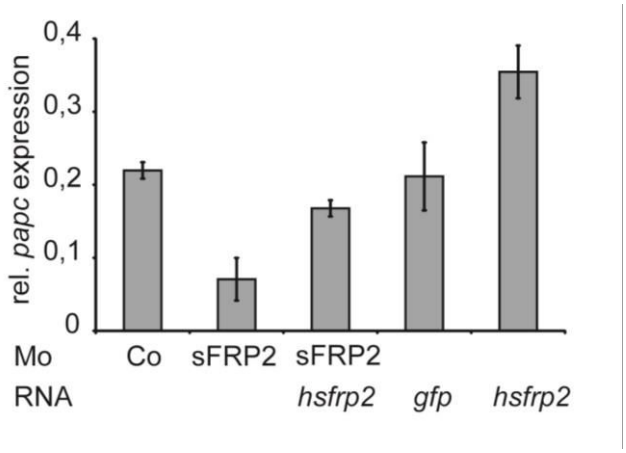

Fig. 11: **sFRP2 is required for *papc* induction during *Xenopus* gastrulation**. Relative expression of *papc* analyzed by qPCR in whole embryos injected with indicated Mos (15 ng) and synthetic mRNA (200pg). Chart shows a representative with technical triplicates confirmed by at least n=2 independent experiments in different batches of *Xenopus laevis* with similar results.

To examine whether sFRP2 is able to enhance Wnt5a/Ror2 signaling directly, I used *Xenopus* AC explants and examined the induction of *papc* in the presence of sFRP2. In wt ACs excised at blastula stage Ror2 and Wnt5a are not expressed endogenously and only very few transcripts of *papc* can be detected. Ectopic expression of Ror2 and Wnt5a is known to induce the transcription of *papc* in AC explants (Schambony and Wedlich, 2007). By co-injection of *sfrp2* mRNA in the AC, I could show that sFRP2 strongly enhanced Wnt5a/Ror2 mediated *papc* expression compared to the level induced by Wnt5a/Ror2 alone (Fig. 12). This up-regulation of *papc* strictly depends on the presence of Wnt5a since co-expression of sFRP2 and Ror2 alone could not induce *papc* (Fig. 12).

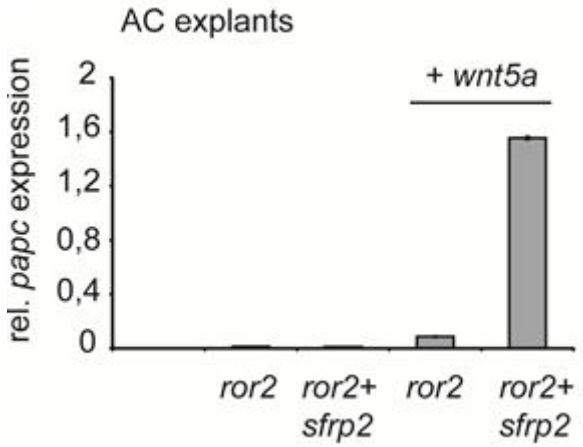

Fig. 12: **sFRP2 enhances Wnt5a/Ror2 mediated *papc* expression**. Relative expression of *papc* analyzed by qPCR in AC explants injected with indicated synthetic mRNAs (500pg *ror2/sfrp2* and 150pg *wnt5a*). Chart shows a representative with technical triplicates confirmed by at least 3 independent experiments in different batches of *Xenopus laevis* with similar results.

To confirm the potentiating effect of sFRP2 on Ror2 signaling, I further used the ATF luciferase reporter assay, which is based on JNK dependent phosphorylation and therefore serves a readout system for β-catenin independent Wnt signaling. In line with my previous observation, sFRP2 augmented Wnt5a/Ror2 mediated ATF activity (Fig. 13). Taken together, these findings demonstrate that sFRP2 is required for *papc* expression during *Xenopus* gastrulation and acts as a positive modulator for Ror2 mediated signaling.

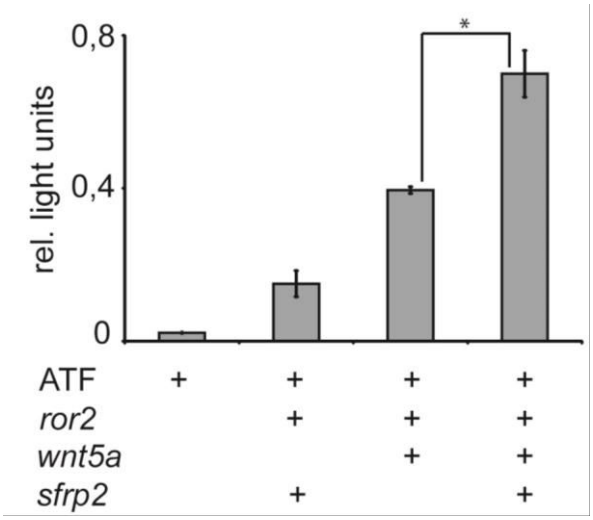

Fig. 13: **sFRP2 enhances Ror2 induced non-canonical Wnt signaling**. ATF luciferase reporter assay of stage12 gastrula embryos injected with the indicated synthetic mRNAs (500pg *ror2/sfrp2* and 100pg *wnt5a*) and the ATF2 luc and TK Renilla reporter constructs. Graph shows the mean ± SD of biological triplicates of pools of 7 embryos each (* $p < 0.05$ to controls). This was confirmed in at least n=3 independent experiments in different batches of *Xenopus* laevis.

3.3 sFRP2 interacts with Ror2 via its CRD and stabilizes Wnt5a/Ror2 complexes

To investigate whether the molecular mechanism underlying the observed positive modulation of Wnt5a/Ror2 signaling by sFRP2 occurs via interaction of sFRP2 with the ligand/receptor complex, I performed binding studies in Hek293 cells. For this purpose, cells were transfected either alone with Ror2-myc or together with sFRP2-HA. After cells were lysed, protein lysates were further incubated with corresponding antibodies and purified with magnetic beads. In western blot analysis, I could show that sFRP2 physically interacts with Ror2 (Fig. 14).

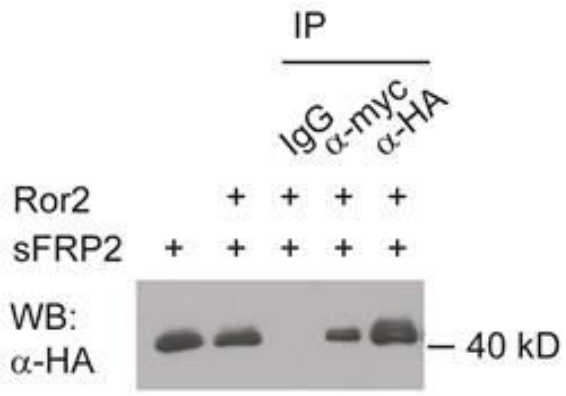

Fig. 14 : **sFRP2 interacts with Ror2 in HEK293T cells.** CO-IP in Hek293 cells transfected with Ror2-myc and HA-tagged sFRP2 (1µg each). Protein lysates were precipitated with antibody against myc or HA, respectively, and IgG as negative control. Western Blot (WB) analysis with anti-HA antibody shows that sFRP2 is pulled down together with Ror2.

Previously, it was demonstrated that association of Fz7 with Ror2 enhances the affinity of Wnt5a to Ror2 and is required for Wnt5a/Ror2 signaling to induce the activation of AP-1 (JNK/c-jun) (Nishita et al., 2010). Since the CRDs of Fz receptors and sFRPs are homologous, I tested whether sFRP2, similar to Fz7, can enhance Wnt5a binding to Ror2. Hek293 cells were either transfected with Ror2 alone or co-transfected with sFRP2, sFRP2-CRD or Fz7 as a positive control. After stimulating the cells with equal amounts Wnt5a conditioned medium, I compared the levels of bound Wnt5a that co-precipitated with Ror2. In the absence of Fz-CRD containing proteins, only traces of Wnt5a were associated with Ror2 (Fig. 15A). However, when sFRP2 or its CRD were co-expressed, significantly more Wnt5a co-precipitated with Ror2. This increase was even stronger than the increase observed in the presence of Fz7 (Fig. 15A). However, this is not surprising because also more sFRP2 and sFRP2-CRD precipitated with Ror2 compared to Fz7 (Fig. 15B). As a control protein containing an unrelated cysteine-rich domain we used Dkk3 (Fig. 15C), which does not bind to Ror2 (Fig.15B) and hence did not increase Wnt5a binding to Ror2 (Fig. 15A).

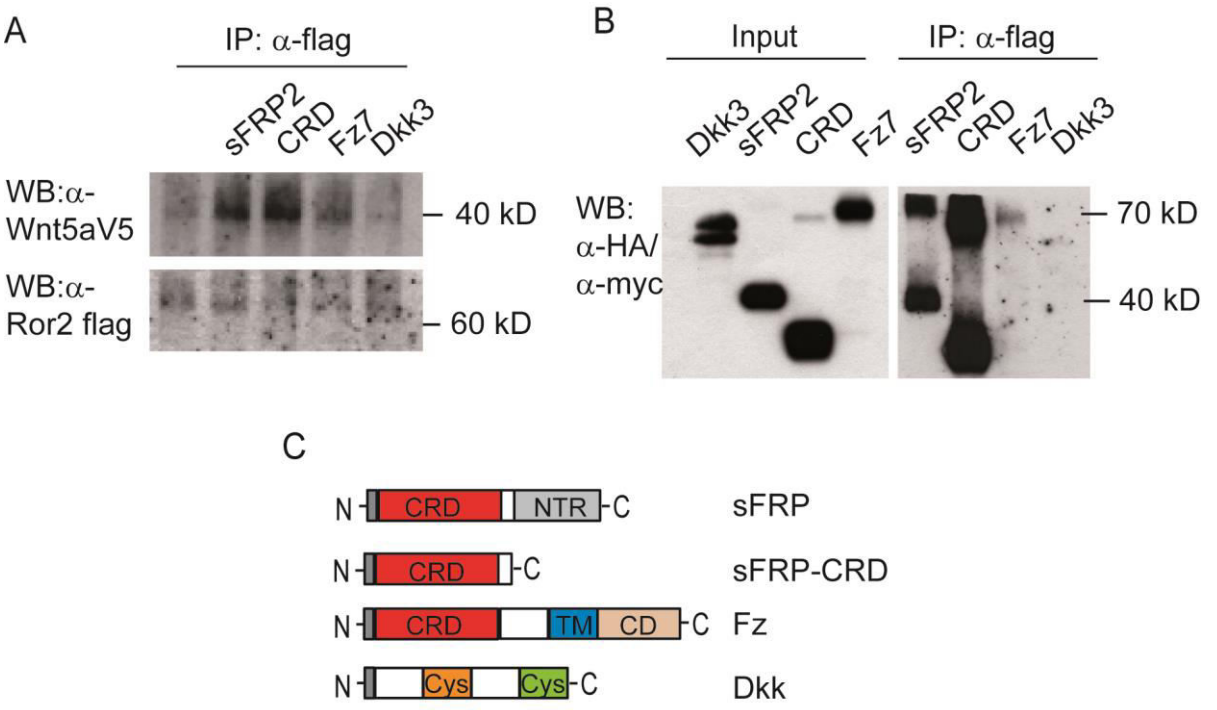

Fig. 15: sFRP2 stabilizes Wnt5a/Ror2 complexes in Hek293 cells. A: The Wnt5a-V5 binding assay was performed in Hek293 cells transfected with Ror2 ECD-flag alone or co-transfected with sFRP2-HA, CRD-HA, DKK3-HA or Fz7-myc (1µg each). Each cell sample was treated with equal amounts of Wnt5a-V5 conditioned medium for 20 min before cells were lysed for anti-flag pull-down to precipitate Ror2. Two different WB analyses were performed: WB on top was analyzed with anti-V5 antibody and shows the Wnt5a-V5 fraction bound to precipitated Ror2 flag. The bottom WB was analyzed with anti-flag and shows that equal amounts of Ror2 were precipitated in the different samples. **B:** The WB analyzed with anti-HA and anti-myc antibody shows that all co-transfected proteins were expressed (Input, first 4 lanes) and were co-precipitated with the Ror2 flag pull-down (IP: anti-flag, last 4 lanes). Only Dkk3 was not precipitated with Ror2. **C**: A scheme of the different proteins used in the experiment. sFRP family proteins are related to Fz receptors in the CRD. CRD: Cysteine-rich domain; NTR: netrin-like domain; TM: Transmembrane domain; CD: cytoplasmic domain; Cys: Cysteine-rich domain.

The stabilizing effect of sFRP2 on Wnt5a was further confirmed *in vivo* using fluorescently tagged proteins in zebrafish embryos. In the absence of sFRP2 only a low level of Wnt5a-GFP co-localized with Ror2-mCherry at the membrane (Fig. 16). However, co-expression of sFRP2 increased co-localization of Ror2 with Wnt5a in punctae at the plasma membrane (Fig. 16). Taken together, our data suggests that sFRP2 specifically binds to Ror2 via its CRD and thereby increases the recruitment of Wnt5a to Ror2 receptor complexes at the plasma membrane, as indicated by stabilized Wnt5a/Ror2 complex formation.

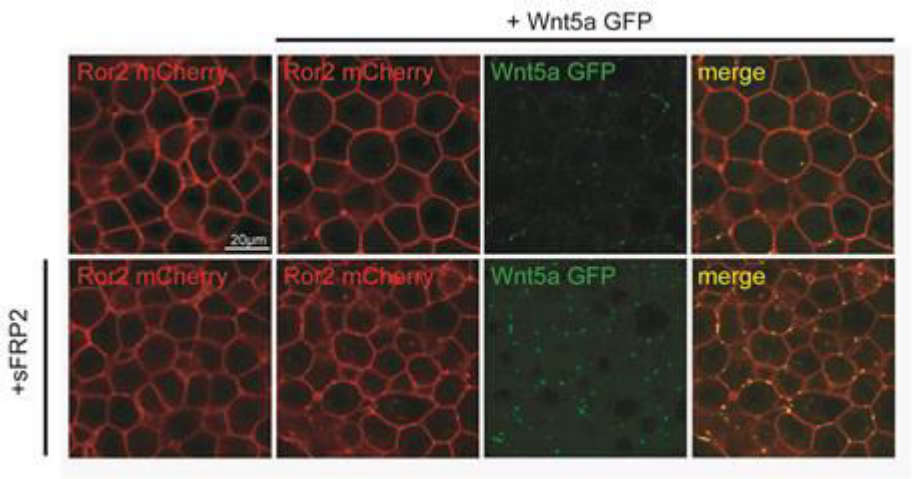

Fig. 16: **sFRP2 stabilizes Wnt5a/Ror2 complexes in zebrafish embryos.** Confocal microscopy analysis of live zebrafish embryos expressing 1ng mRNA of the indicated constructs at 30-50% epiboly stages shown in the indicated colors. Confocal images represent single z sections. Ror2 shows membrane localization regardless of the presence of Wnt5a or sFRP2. Wnt5a shows co-localization with Ror2 in discrete clusters at the membrane. Co-expression of sFRP2 with Ror2/Wnt5a leads to an enhanced membrane localization of Wnt5a. (Result obtained in collaboration with Benjamin Mattes from the Scholpp Lab, ITG, KIT).

3.4 sFRPs and Fz7 act redundantly in Ror2 activation

We showed that the sFRP2-CRD mediates interaction with Ror2 and is able to enhance Wnt5a/Ror2 complex formation. The CRD of sFRP2 is highly homologous to those of other secreted Wnt modulators of the sFRP family. Thus, I analyzed whether other sFRPs are also involved in *papc* transcription. Indeed, a knock-down of sFRP1 and frzb2 reduced the expression of *papc* compared to control embryos, suggesting that sFRP1 and frzb2 also positively modulate Ror2 signaling (Fig. 17A). In contrast, knockdown of Dkk1, a secreted modulator of Wnt/β-catenin signaling, had no influence on the expression of *papc* (data not shown). Moreover, I observed that frzb2 could rescue the sFRP2 Mo phenotype (Fig. 17B), indicating that they can function redundantly to induce *papc*.

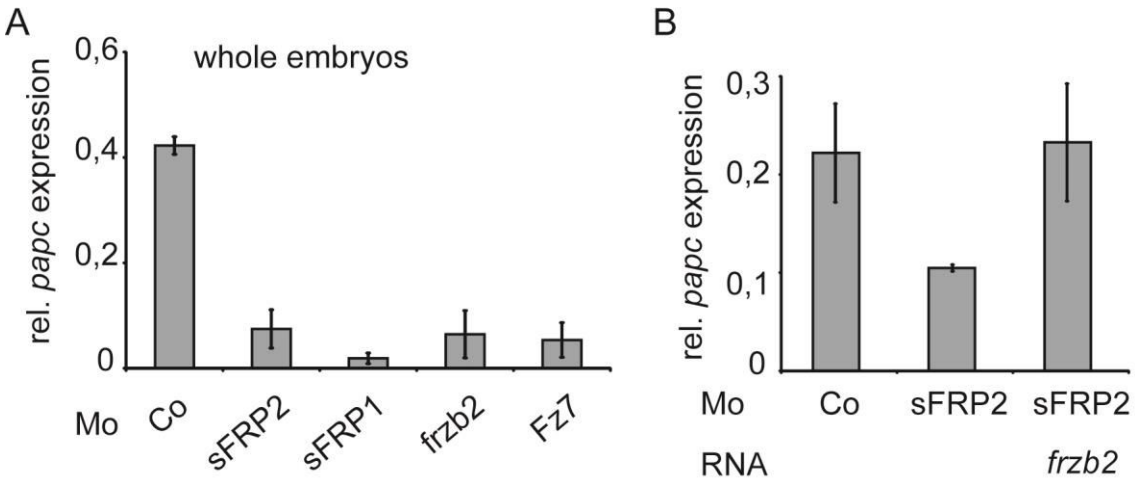

Fig. 17: **sFRP1, frzb2 and Fz7 are also required for *papc* expression**. **A+B:** Relative expression of *papc* analyzed by qPCR in gastrula stage 10.5 embryos injected dorsal equatorially with indicated Mos (15ng) and mRNA (200pg *frzb2).* **A:** Loss of sFRP2, sFRP1, frzb2 and Fz7 by dorsal Mo injection reduces *papc* induction at gastrula stage. **B:** Coinjection of frzb2 mRNA can rescue Mo mediated loss of sFRP2. Charts show a representative with technical triplicates confirmed by at least 3 independent experiments in different batches of *Xenopus laevis* with similar results.

Consistent with my hypothesis that Fz-CRDs enhance Wnt5a/Ror2 signaling, knockdown of Fz7 reduced the level of *papc* in qPCR (Fig.17A.) and in whole mount *in situ* hybridization experiments (Fig. 18A). Loss of Fz7 therefore mimics loss of sFRP2 and Ror2. This suggests that both receptors also co-operate *in vivo*, in line with the known role of Fz7 in Wnt5a/Ror2 induced AP-1 activation *in vitro* (Nishita et al., 2010).Consequently, I investigated whether Fz7 has an effect on Ror2 induced signaling in AC explants and found that Wnt5a/Ror2 mediated induction of *papc* is further enhanced by co-injection of *fz7* mRNA (Fig. 18B). Notably, in the absence of Ror2, Fz7 was unable to induce *papc* expression in AC, confirming that *papc* is a Ror2 specific target gene, as published earlier (Schambony and Wedlich, 2007). I hypothesize that the presence of a CRD motif is required to stabilize the Wnt5a/Ror2 signaling complex irrespective if provided by the Fz7 receptor or secreted Fz-related modulators.

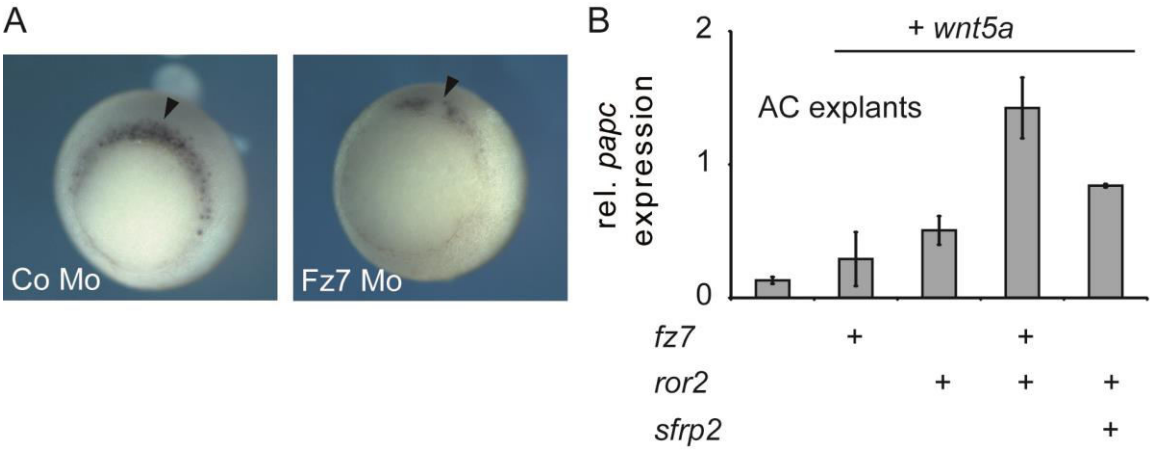

Fig. 18: **Fz7 is required for *papc* expression. A:** *papc* expression of Fz7 morphants analyzed by whole mount *in situ* hybridization of gastrula stage embryos. Arrowheads indicate site of injection. **B:** Relative expression of *papc* analyzed by qPCR in AC explants injected with indicated synthetic mRNAs (500pg *ror2*/*fz7* and 150pg *wnt5a*). Chart shows a representative with technical triplicates confirmed by at least 3 independent experiments in different batches of *Xenopus laevis* with similar results.

3.5 sFRP2 and Ror2 inhibit Fz7 mediated signaling

Gastrulation movements during *Xenopus* development are not only affected by the Wnt5a/Ror2 mediated signaling (Schambony and Wedlich, 2007; Seitz et al., 2014; Torres et al., 1996; Veeman et al., 2003; Wallingford et al., 2002) . As described earlier, Fz7 also activates non-canonical Wnt signaling when stimulated with Wnt5a or Wnt11 (Habas et al., 2003; Kim et al., 2008) and due to the known role of sFRPs as Wnt signaling modulators (Kawano and Kypta, 2003; Wawrzak et al., 2007), I further analyzed whether sFRP2 acts in the same complex with Fz7 and affects Fz7 signaling activity. Using Co-IP, I could show that in addition to Ror2 (Fig. 14), sFRP2 also interacts with Fz7 (Fig. 19).

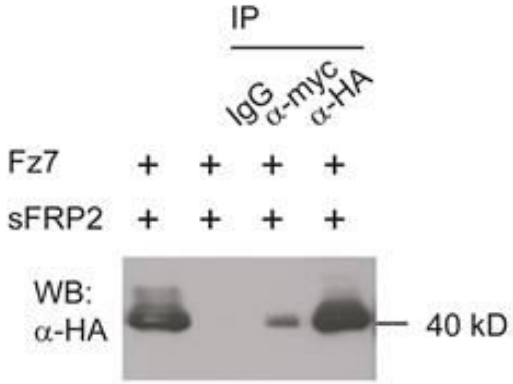

Fig. 19: **sFRP2 physically interacts with Fz7 *in vitro*.** CO-IP in Hek293 cells transfected with Fz7-myc and sFRP2-HA (1µg each). Protein lysates were precipitated with antibody against myc or HA respectively and IgG as negative control. Western Blot (WB) analyzed with anti-HA antibody shows that sFRP2 is pulled down together with Fz7.

Since no specific target gene analysis, like *papc* for Ror2 signaling, is known so far for Fz7 mediated signaling, I used a chimeric NT7C5 receptor construct (Swain et al., 2001). This chimeric receptor consists of the extracellular- and transmembrane domains of Fz7, which Wnt5a or Wnt11 bind to and the intracellular domain of human Fz5, which transmits the canonical Wnt signal upon ligand binding. Therefore this receptor induces the expression of the Wnt/ β-catenin target gene Nodal-related (*xnr3*), when stimulated with Wnt5a. In contrast, wt *Xenopus* Fz7 cannot activate *xnr3* after Wnt5a stimulation. Analysis of the *xnr3* expression in NT7C5 injected AC explants by qPCR revealed that sFRP2 (Fig. 20) inhibits Wnt5a/NT7C5 induced *xnr3* expression. The inhibitory effect mediated by sFRP2 was also observed when Wnt11, an alternative ligand for Fz7, was used instead of Wnt5a (data not shown).

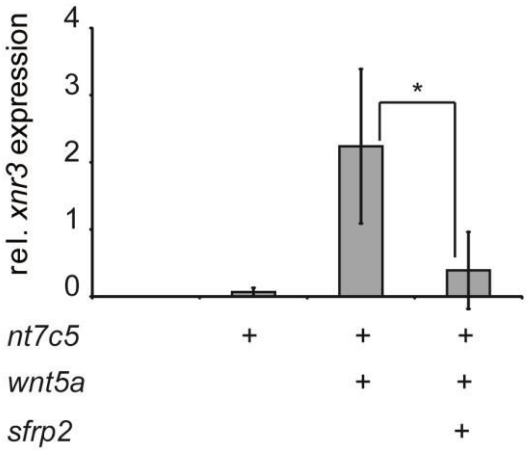

Fig. 20: **sFRP2 inhibits NT7C5 mediated *xnr3* expression.** qPCR analysis of AC explants of embryos injected with the indicated mRNAs (500pg *n7c5/sfrp2* and 100pg *wnt5a*) Charts shows the mean ± SD of n=3 independent experiments (*) indicates significant difference (Student´s *t* test* p<0.05, **p<0.001) compared to controls.

Previous data have shown that apart from its interaction with Ror2 the Fz7 receptor can also induce Ror2-independent Wnt/PCP signaling (Habas et al., 2003). Thus, I examined whether Ror2 has an influence on Fz7 mediated signaling using the chimeric construct. I quantified *xnr3* expression in NT7C5/Ror2 injected AC explants and observed that Ror2 completely blocked Wnt5a/NT7C5 mediated *xnr3* induction

(Fig. 21A). To confirm that Ror2 inhibits Fz7 on the receptor level via direct interaction and not by its downstream signaling activity, I included a Ror2 kinase dead (KD) mutant in this assay. Since Fz7 and Ror2 interact via their extracellular CRD, this Ror2 mutant should still form a complex with NT7C5 but has no signaling activity. As demonstrated (Fig.21A), the KD mutant of Ror2 is still able to inhibit NT7C5 induced *xnr3* expression, indicating that the inhibition of Fz signaling is independent of Ror2 downstream signaling. As expected, *papc* expression was not induced by Ror2 KD (Fig. 21B). However, co-expression of wt Ror2 and NT7C5 strongly enhanced Ror2 mediated *papc* expression compared to the *papc* signal induced by Ror2 alone (Fig. 21B), supporting the idea that the extracellular portion of Fz7 is sufficient for enhancing Ror2 signaling.

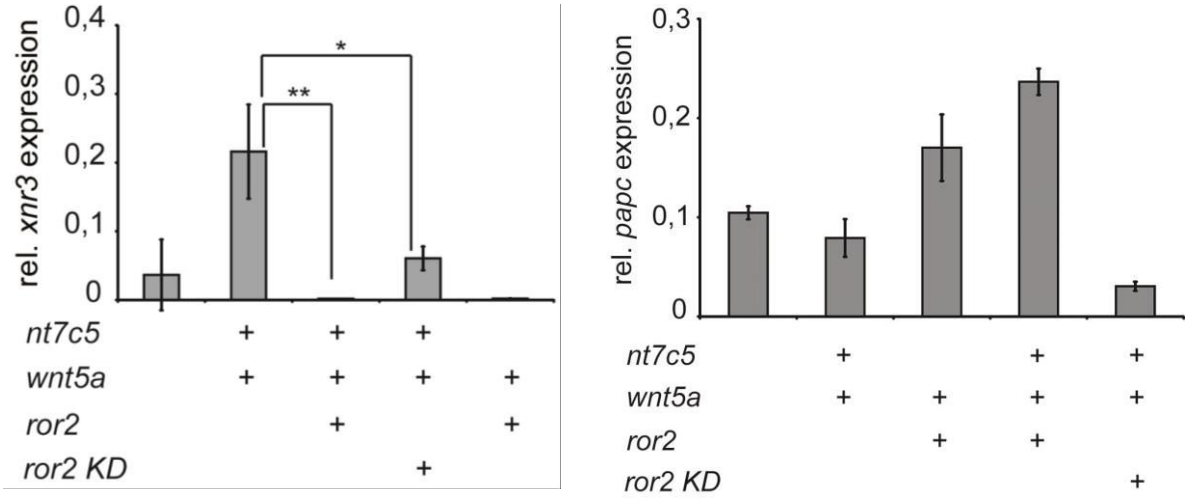

Fig. 21: **Ror2 inhibits NT7C5 mediated *xnr3* expression, while NT7C5 augments Ror2 mediated *papc* expression. A+B:** qPCR analysis of AC explants of embryos injected with the indicated mRNAs (500pg *n7c5/ror2/ror2 kd* and 100pg *wnt5a*). A: Analysis of *xnr3* expression. Chart shows the mean ± SD of three independent experiments (*) indicates significant difference (Student´s *t* test*p <0.05, **p<0.001) compared to controls. **B:** Analysis of *papc* expression. Chart shows a representative with technical triplicates confirmed by n=2 independent experiments in different batches of *Xenopus laevis* with similar results.

To further confirm that sFRP2 and Ror2 are negative regulators for Fz7, I used the ATF-Luc assay. Consistent with my previous observation, that sFRP2 inhibits NT7C5 induced *xnr3* expression; I showed that sFRP2 inhibits Wnt5a/Fz7 mediated ATF reporter activity (Fig. 22A). Since the ATF reporter cannot discriminate between Fz7 and Ror2 induced signaling, I used the Ror2 KD construct, which is not able to

activate the ATF reporter but still binds Fz7. Like sFRP2, also Ror2 KD inhibited Wnt5a/Fz7 induced reporter activity (Fig. 22B).

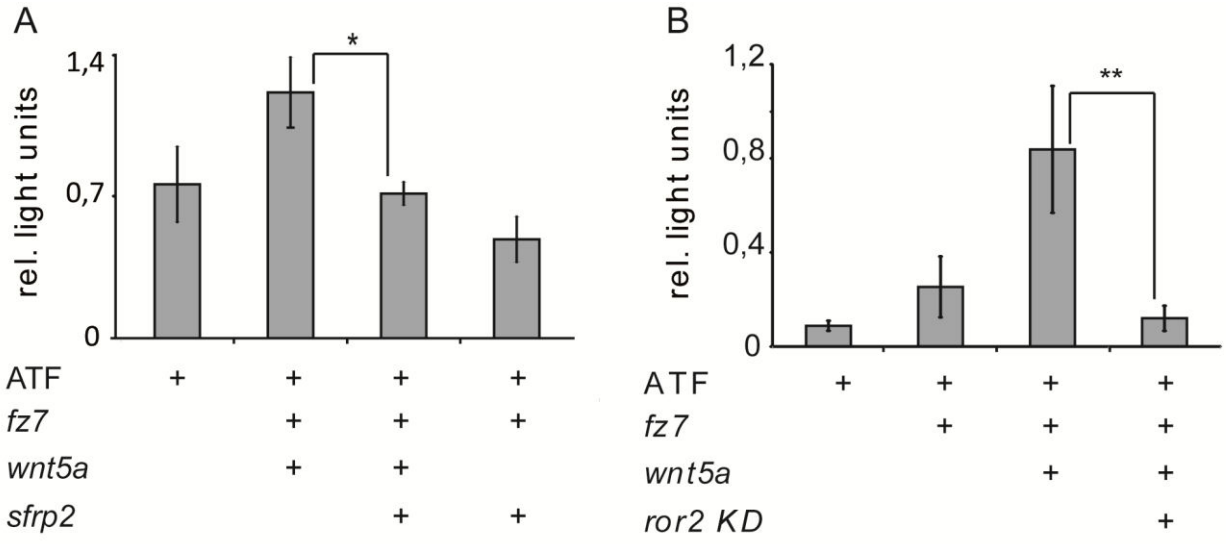

Fig. 22: **sFRP2 and Ror2 inhibit Wnt5a/Fz7 mediated ATF reporter activation. A+B**: ATF luciferase reporter assay of stage12 gastrula embryos injected with the indicated synthetic mRNAs (300 pg *fz7/ sfrp2 / ror2 kd* and 100pg *wnt5a per embryo*) and the ATF luc and TK Renilla reporter constructs. **A**: Co-expression effect of sfrp2. **B:** Co-expression effect of ror2 kd. Graphs show the mean of 3 ± SEM of biological triplicates of pools of 5 embryos each (* p <0.05 to controls). This was confirmed in at least n=3 independent experiments in different batches of *Xenopus* laevis.

Furthermore, a Ror2 KD was also able to inhibit Wnt11/Fz7 induced signaling (Fig. 23). Taken together, my results show that sFRP2 and Ror2 negatively influence Fz7 mediated signaling, while at the same time Ror2 mediated signaling is promoted by Fz7 and sFRP2.

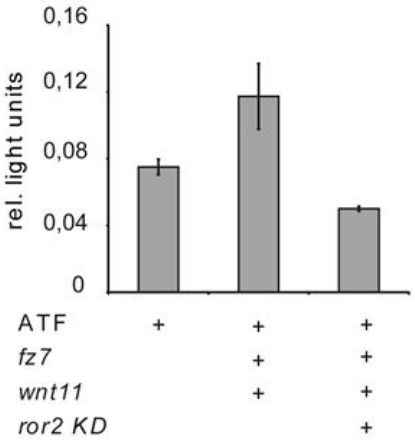

Fig. 23: **Ror2 inhibits Wnt11/Fz7 mediated non-canonical signaling.** ATF luciferase reporter assay of stage12 gastrula embryos injected with the indicated synthetic mRNAs (300 pg *fz7/ror2 kd*

and 100pg *wnt11 per embryo*) and the ATF luc and TK Renilla reporter constructs. Graph shows the mean of 3 ± SEM of biological triplicates of pools of 5 embryos each (* $p < 0.05$ to controls). This was confirmed in at least three independent experiments in different batches of *Xenopus* laevis with similar results.

3.6 sFRP2 and Ror2 inhibit Fz7 induced PKCδ but not PKCα recruitment

In addition to the activation of JNK, Fz7 was shown to trigger membrane recruitment of PKCδ and PKCα. PKCδ plays an essential role in non-canonical Wnt signaling and in the regulation of CE movements (Kinoshita et al., 2003). Unlike PKCα, PKCδ belongs to the family of novel protein C kinases and is not activated through Ca^{2+} molecules (Toker, 1998). Since my data revealed that sFRP2 as well as Ror2 inhibit Fz7 activity, I tested whether they also affect Fz7 mediated recruitment of PKCδ–GFP in *Xenopus* animal cap explants. I expressed either PKCδ–GFP with Fz7 alone, or together with Ror2 or sFRP2 in the animal region of a 2-cell stage embryo. Consistent with published data, PKCδ was translocated to the plasma membrane when co-expressed with Fz7 and indeed both sFRP2 as well as Ror2 disturbed Fz7 induced PKCδ membrane recruitment (Fig. 24). My findings showed that sFRP2 and Ror2 prevent Fz7 receptor mediated PKCδ recruitment.

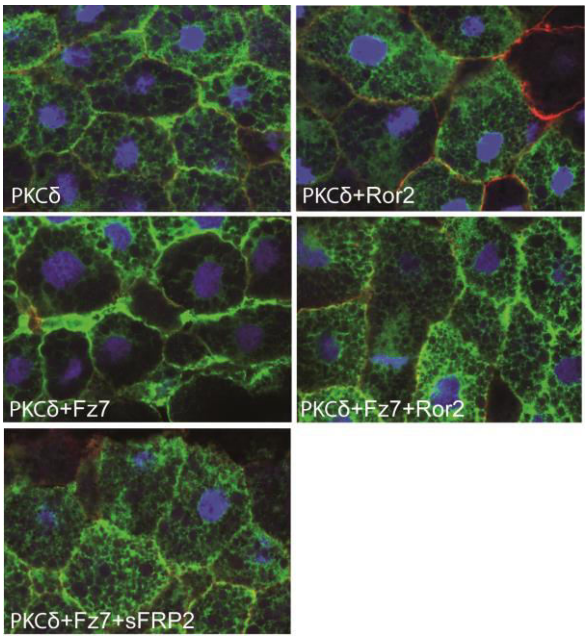

Fig. 24: **sFRP2 and Ror2 inhibit Fz7 induced PKCδ-GFP membrane recruitment.** Confocal microscopy analysis of *Xenopus* animal cap explants expressing indicated mRNAs (500pg PKCδ-GFP

(green), Fz7, Ror2, sFRP2) and 300pg mRNA of the membrane marker mbRFP. To visualize the nucleus, explants were stained with DAPI.

In addition to classical Wnt/PCP signaling, Fz7 also mediates Wnt/Ca^{2+} signaling which involves the activation and membrane recruitment of PKCα, a classical protein C kinase which is activated in response to Ca^{2+} (Winklbauer et al., 2001). Thus, I also examined whether sFRP2 and Ror2 are capable to inhibit Fz7 mediated PKCα-GFP translocation. In the presence of Fz7, PKCα-GFP was recruited to the plasma membrane but neither a co-expression of sFRP2 nor Ror2 inhibited membrane localization of PKCα (Fig. 25). Taken together, my findings suggest that sFRP2 and Ror2 specifically inhibit the Wnt/PCP branch but not Fz7 mediated Wnt/Ca^{2+} signaling.

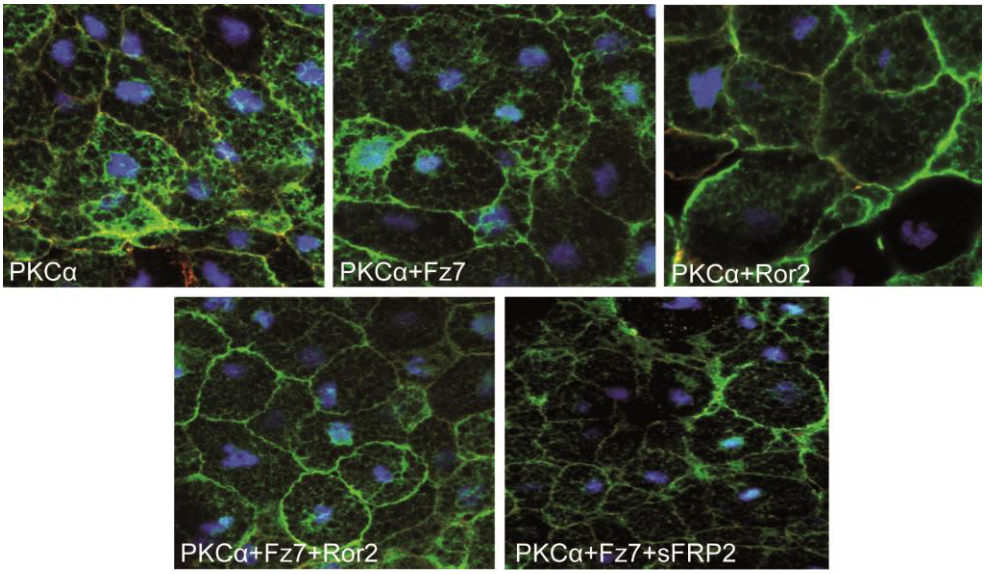

Fig. 25: **sFRP2 and Ror2 do not inhibit Fz7 induced PKCα-GFP membrane recruitment.** Confocal microscopy analysis of *Xenopus* animal cap explants expressing indicated mRNAs (500pg PKCα-GFP (green), Fz7, Ror2, sFRP2). To visualize the nucleus, explants were stained with DAPI.

3.7 sFRP2 and Ror2 prevent Fz7 receptor endocytosis

A recent study demonstrated that the internalization of Fz4 via clathrin-mediated endocytosis is required for non-canonical Wnt signaling (Chen et al., 2003). This is supported by the finding that activation of Rac by Wnt5a requires the internalization of Fz2 (Yu et al., 2010) and results suggest that the endocytosis is an essential step for transducing the non-canonical Wnt signal. Since my data showed that sFRP2 and

Ror2 are inhibitors for the Fz7 receptor, I analyzed whether they have an effect on the localization of Fz7 and might block Fz7 internalization. In Hek293 cells, I first observed that the over-expression of Ror2 and sFRP2 resulted in a stronger accumulation of Fz7 protein at the cell membrane.

Therefore, I next analyzed whether a loss of sFRP2 or Ror2 have an effect on Fz7-GFP localization in *Xenopus* and injected antisense morpholino oligonucleotides for sFRP2 or Ror2 into the dorsal marginal zone (DMZ) of 4-cell stage embryos. Fluorescence immunostainings show that loss of sFRP2 or Ror2 only slightly affected localization of Fz7-GFP (Fig. 26A). When Fz7-GFP was expressed alone it was more continuously expressed at the membrane. However, I always observed few more Fz7-GFP vesicles when Wnt5a or morpholinos for sFRP2 or Ror2 were co-injected (Fig. 26A). These data indicate that sFRP2 and Ror2 might prevent Fz7 receptor endocytosis. However, immunostainings of Fz7-GFP in *Xenopus* explants were very difficult to interpret since no clear Fz7 vesicles were formed and membrane localization was not significantly reduced by Wnt5a stimulation. Over-expressed Fz7-GFP was always localized in a diffuse pattern inside the cell and partially trapped in the ER (Fig. 26A). To confirm that sFRP2 and Ror2 are involved in blocking Fz7 endocytosis, I overexpressed sFRP2 or Ror2 in the animal hemisphere together with Fz7-GFP and Wnt5a. Co-expression of Wnt5a should stimulate the endocytosis of Fz7-GFP, which I expected to be inhibited by sFRP2 or Ror2 over-expression. However, co-injection of Wnt5a alone did not lead to a significant decrease of Fz7-GFP at the plasma membrane or an increase of Fz7-GFP positive vesicles (Fig. 26B), indicating that Wnt5a stimulation did not work as expected. Nevertheless, both, sFRP2 and Ror2 co-expression resulted in a stronger accumulation of Fz7-GFP protein at the cell membrane (Fig. 26B). Therefore, these finding confirm the trend found in the loss of function analysis in the DMZ (Fig. 26A) and support my hypothesis that sFRP2 and Ror2 interfere with Fz7 receptor internalization.

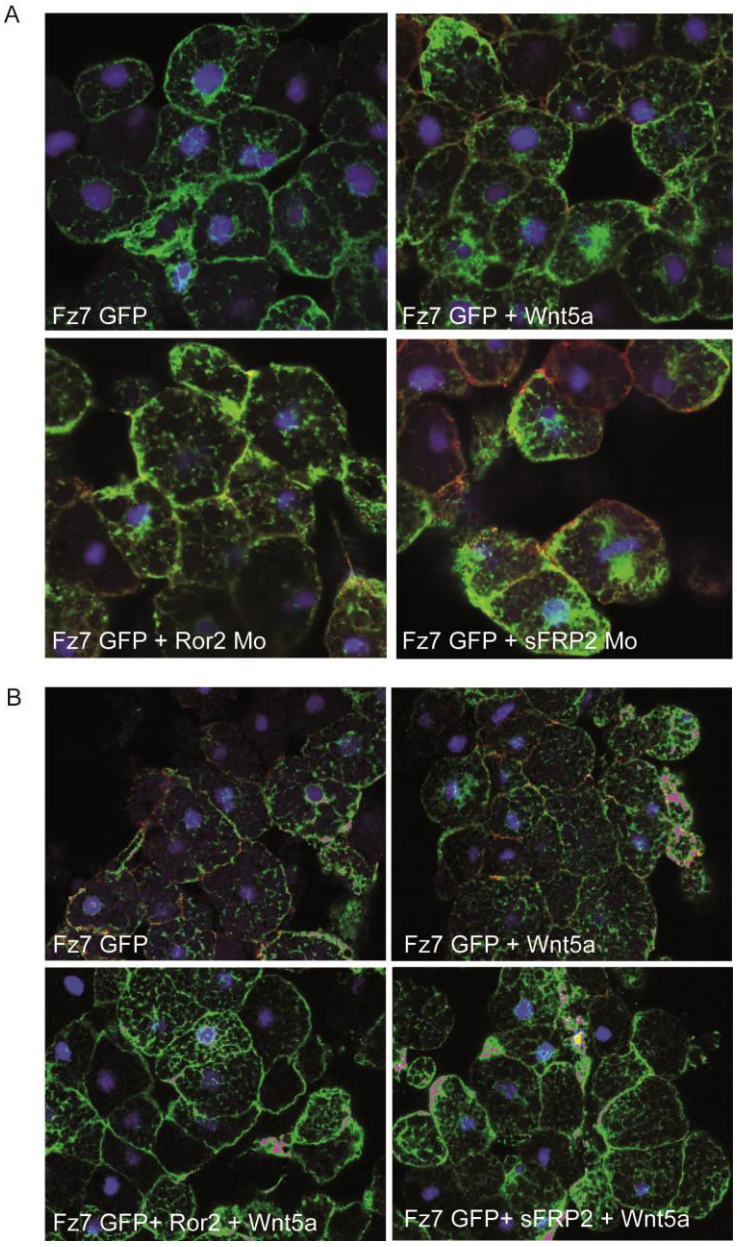

Fig. 26: **sFRP2 and Ror2 prevent Fz7 receptor internalization in *Xenopus***. Confocal microscopy analysis of *Xenopus* DMZ explants for loss-of-function **(A)** and AC explants for gain of function **(B)** effects. The embryos were injected at 2-4 cell stage in the area of explantation with 500pg of the indicated constructs, 15 ng of the indicated morpholinos and 300pg mRNA of the membrane marker mbRFP. To visualize the nucleus, explants were stained with DAPI.

Although both gain and loss of function analysis in the *Xenopus* explants already point towards an inhibitory function of sFRP2 and Ror2 on Wnt5a induced Fz7 endocytosis, the data obtained involved technical problems, which will be discussed later. Therefore, I additionally tested whether a knockdown of sFRP2 or Ror2 also affects the localization of endogenous Fz7 protein in DMZ explants. Compared to explants that were injected with a Co Mo, loss of sFRP2, Ror2 as well as a double

knockdown of both proteins clearly reduced Fz7 membrane localization (Fig. 27). A similar effect was observed when explants were treated with Wnt5a. These findings indicate that sFRP2 and Ror2 are required for Fz7 membrane stabilization.

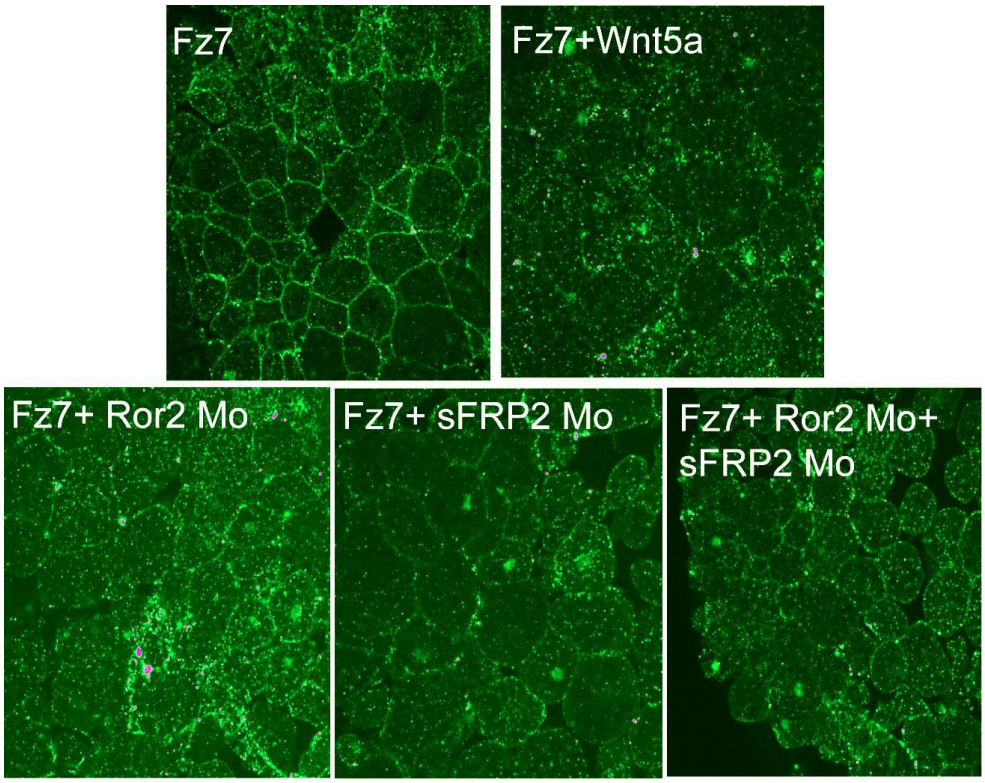

Fig. 27: Loss of sFRP2, or Ror2 and a double knockdown of both proteins reduce endogenous Fz7 membrane localization. Confocal microscopy analysis of Xenopus DMZ explants. The embryos were injected at 4-cell stage in the the dorsal equatorial zone with 500pg Wnt5a and 15 ng of indicated morpholinos.

To confirm the trend observed in the *Xenopus* explants, I decided to include microscopic analyses in zebrafish, as another vertebrate model system.

High-resolution *in vivo* imaging in zebrafish embryos has recently proven a valuable tool to study trafficking of Wnt ligands and receptors in a living vertebrate model organism (Hagemann et al., 2014; Stanganello et al., 2015). By using this imaging-based *in vivo* approach performed in the lab of Steffen Scholpp (KIT, ITG, Karlsruhe, Germany), we observed that in the absence of Wnt5a, Fz7 (Fz7-CFP) was localized at the cell membrane as well as in intracellular vesicles. After stimulation with Wnt5a, Fz7 was translocated from the membrane to intracellular vesicles (Fig. 28). However, co-injection of sFRP2 or Ror2 (Ror2-mCherry) decreased Wnt5a induced Fz7 receptor internalization. Instead, Ror2-mCherry and Fz7-CFP molecules formed

prominent clusters at the plasma membrane upon Wnt5a stimulation (Fig. 28). When sFRP2, instead of Ror2, was co-expressed along with Fz7 and Wnt5a, cluster formation of Fz7 was not observed (Fig. 28). Moreover, cluster formation was dependent on the presence of Wnt5a, since Fz7 and Ror2 alone did not form clusters. In the absence of Wnt5a or Ror2, Fz7 was homogenously distributed at the membrane. Collectively, these findings confirm the data obtained in *Xenopus* and indicate that sFRP2 and Ror2 trap Fz7 at the cell membrane, probably to reduce Fz7 receptor internalization and signaling.

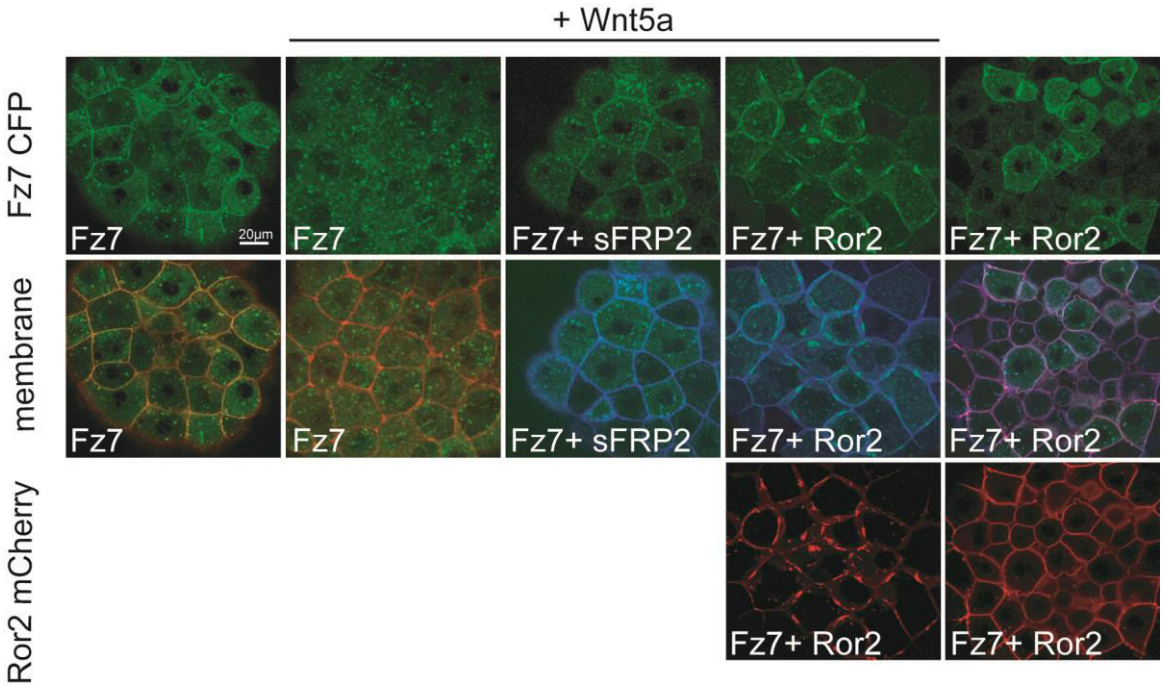

Fig. 28: **sFRP2 and Ror2 prevent Fz7 receptor internalization in zebrafish.** Confocal microscopy analysis of live zebrafish embryos expressing 1ng mRNA of indicated constructs at 30% - 50% epiboly stage together with 1ng mRNA of the membrane marker mem-mCherry (red) or GFP-GPI (blue). Fz7-CFP (green) is present at the membrane and in endocytic vesicles. Co-expression of Wnt5a leads to enhanced internalization. sFRP2 as well as Ror2 are able to decrease Wnt5a mediated endocytosis of Fz7.

It is conceivable that in complex with Fz7, with the transmembrane protein Ror2 serves as an anchor, which blocks endocytosis. For soluble sFRP2 this mechanism is less obvious. Interestingly, the NTR domain of sFRP was suggested to interact with heparan proteoglycans at the cell membrane (Finch et al., 1997). To investigate if the NTR is responsible for sFRP association with the cell membrane, I analyzed Fz7 localization in the presence of the NTR deletion mutant. Indeed, I found that

sFRP2 lacking the NTR domain was less potent in stabilizing Fz7 at the membrane (Fig. 29).

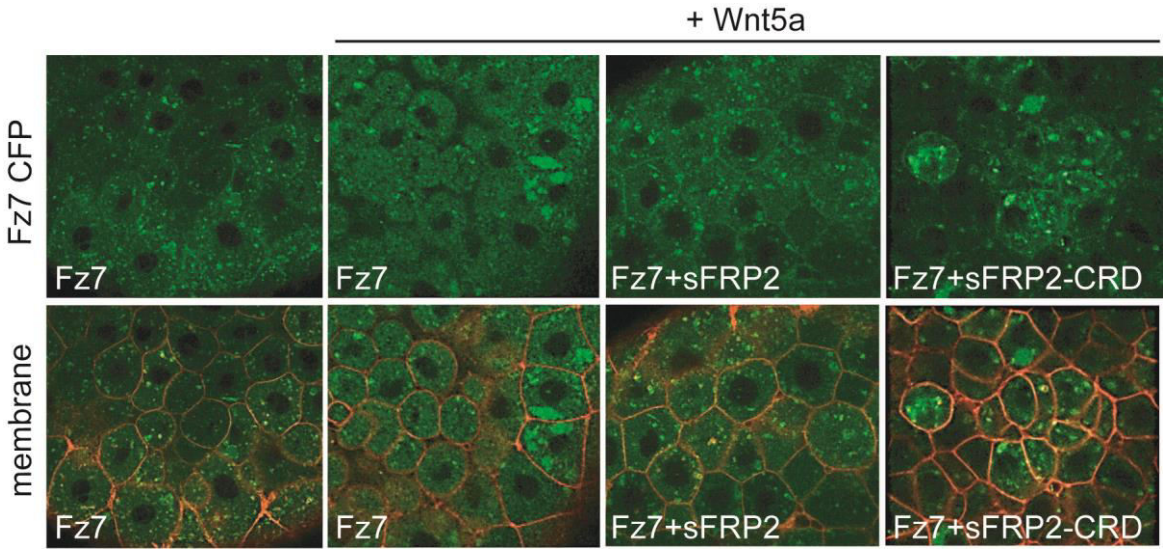

Fig. 29: **sFRP2 lacking the NTR domain does not prevent Fz7 membrane internalization in zebrafish**. Confocal microscopy analysis of live zebrafish embryos expressing 1ng mRNA of indicated constructs at 30% - 50% epiboly stage together with 1ng mRNA of the membrane marker mem-mCherry (red). Fz7-CFP (green) is present at the membrane and in endocytic vesicles. Co-expression of Wnt5a leads to enhanced internalization, which is repressed by full length sFRP2 (also compare with Fig.28). The CRD of sFRP2 alone is unable to prevent Wnt5a induced stabilization of Fz7 at the membrane but appears to increase size of the Fz7 vesicles.

Taken together, my data support a novel role for sFRPs on the activation of distinct branches of the non-canonical signaling network. sFRPs activate Wnt5a/Ror2 signaling by stabilizing the ligand/receptor complex and have an inhibitory effect on Fz7 mediated signaling, most likely by inhibiting its endocytosis. While the CRD of sFRP2 seems to be sufficient for the activation of the Wnt5a/Ror2 pathway, the NTR domain seems to be essential for efficient Fz7 receptor stabilization. My data further indicate that sFRP2 as well as Ror2 specifically inhibit Fz7 mediated PKCδ but not PKCα recruitment suggesting that they have modulating functions in Wnt/PCP but not Wnt/Ca^{2+} signaling.

4 Discussion

4.1 Co-expression of Ror2 and Fz7 leads to selective pathway inhibition or activation

A tight regulation of the different Wnt signaling cascades is crucial for proper cell migration during embryonic development. During *Xenopus* development, the receptors Fz7 and Ror2 are stimulated by the same ligand, but can activate different downstream effectors and are suggested to mediate two distinct branches of β-catenin independent Wnt signaling (Fig. 4) (Ho et al., 2012; Niehrs, 2012; Schambony and Wedlich, 2007). However, it has also been shown that Fz7 and Ror2 co-operate to induce the activation of AP-1 *in vitro* (Nishita et al., 2010). Using specific read-outs for the distinct branches of Ror2 and Fz7, I was able to shed more light on the molecular interplay of these two parallel pathways *in vivo*.

For Ror2 mediated signaling, I analyzed the expression of the target gene *papc* and found that Fz7 enhances Ror2 mediated signaling and is required for *papc* expression during *Xenopus* gastrulation (Fig. 18). This function is independent of the intracellular Fz domain, since a stronger *papc* induction was also observed when the chimeric Fz7 receptor with a “canonical” signaling domain of Fz5 (NT7C5) was co-expressed with Ror2 (Fig. 21). This suggests that the presence of an extracellular Fz-CRD motif promotes Ror2 activity. Surprisingly, signal transduction via the Fz7 receptor is repressed when both receptors are co-expressed. Using the chimeric NT7C5 receptor to monitor Fz7 mediated signaling, I observed that Ror2 inhibited Wnt5a/NT7C5 induced *xnr3* expression (Fig. 21). This inhibition was not caused by downstream signaling components of Ror2, which inhibit Wnt/β-catenin signaling (Yuan et al., 2011), because the kinase inactive Ror2 mutant, Ror2 KD (Fig. 21) (Schambony and Wedlich, 2007), also inhibited NT7C5 signaling. Thus, these data indicate that inhibition of Fz7 signaling by Ror2 occurs at the level of receptor complex formation.

4.2 sFRP2 fine-tunes signaling of Fz7 and Ror2 at the receptor level

Data obtained by characterizing the function of sFRP2 strongly support the assumption that the presence of an extracellular Fz7-CRD motif promotes Ror2 activity. In this study, I demonstrate that sFRP2 is required for morphogenesis during *Xenopus* gastrulation by differentially modulating the Ror2 and the Fz7 pathways. Similar to Ror2, sFRP2 inhibited Wnt5a/Fz7 mediated ATF activation (Fig. 22) as well as Wnt5a/NT7C5 induced *xnr3* expression (Fig. 20) and TopFlash activity. Focusing on Ror2 signal transduction, I found that sFRP2, like Fz7, cooperates with Ror2 to induce Wnt5a mediated *papc* expression (Fig. 12). Moreover, sFRP2 and other sFRPs are required for *papc* expression during gastrulation (Fig. 17), which further supports the hypothesis that CRDs of Fz-related proteins promote and are required for Ror2 signal transduction. Notably, preliminary data revealed that sFRP2 binds to Ror2 via its CRD motif.

Although there are several studies showing that sFRPs can act as Wnt signaling modulators (Bhat et al., 2007; Leyns et al., 1997; Lin et al., 1997; Lopez-Rios et al., 2008; Uren et al., 2000), the mechanism of Wnt signal regulation by sFRPs is still unresolved. Due to my findings I focused on the function of the CRD in this process and provide insights into the potential mechanism of Ror2 signal regulation. Since the CRD of sFRP2 alone was able to enhance Wnt5a binding to Ror2 (Fig. 15A), I suggest that CRDs are responsible for Wnt5a/Ror2 stabilization and enhanced Ror2 signaling. Notably, Dkk3 which contains a cysteine-rich region distinct from those of classical Fz and sFRP CRDs (Cruciat and Niehrs, 2013) did not bind to Ror2 and had no effect on Wnt5a/Ror2 stabilization (Fig. 15). The Fz7 receptor, however, is known to enhance Wnt5a binding to Ror2 (Nishita et al., 2010), indicating that Ror2 signal transduction is specifically affected by Fz CRDs.

The findings, that sFRPs stabilize Wnt5a/Ror2 complex formation, is further consistent with the observation that sFRP2 increased Wnt5a punctae at the plasma membrane in zebrafish embryos (Fig. 16). However, in the absence of sFRP2 there was constantly less Wnt5a-GFP detected in the experiments, which could indicate that Wnt5a-GFP is stabilized upon binding to a CRD of a receptor or a sFRP. In the absence of a CRD motif, Wnt5a might be degraded. This correlates with data showing that Ror2 signaling is much lower when only Wnt5a was co-expressed (Fig.

12). Of note, there was no an additional increase of Ror2 activity using higher concentrations of sFRP2 (data not shown), indicating that sFRP2 might modulate Wnt signaling in a biphasic manner and might form inactive clusters at high concentrations. Consistently, data published previously showed that increasing amounts of soluble mouse Fz8-CRD modulated Wnt3a induced signaling in a biphasic manner and micromolar CRD concentrations were proposed to form inactive Wnt-CRD polymers (Kumar et al., 2014).

Taken together, results show that sFRP2 is necessary to regulate morphogenic movements during *Xenopus* gastrulation. sFRP2 inhibits Fz7 but augments Ror2 signaling suggesting that sFRP2 balances the signaling activities of Ror2 and Fz7. Furthermore, the CRD of sFRP2 is sufficient to stabilize Wnt5a/Ror2 complexes at the membrane and thereby promotes Ror2 signal transduction.

4.3 sFRP2 and Ror2 inhibit Fz7 mediated PKCδ but do not affect Fz7 mediated Wnt/Ca^{2+} signaling

Activation of Fz7 was further shown to trigger the Wnt/Ca^{2+} branch through heterotrimeric G-proteins, which leads to the activation of Ca^{2+} sensitive protein kinase PKCα. In *Xenopus,* stimulation of PKCα results in its translocation to the cell membrane (Wang and Steinbeisser, 2009; Winklbauer et al., 2001). Fluorescence immunostainings revealed that sFRP2 and Ror2 do not inhibit Fz7 mediated PKCα translocation (Fig. 25) and similar to Fz7, Ror2 alone could induce membrane recruitment of PCKα. Notably, it was demonstrated that Wnt5a/Ror2 induced expression of *papc* is unrelated to the Wnt/Ca^{2+} branch since *papc* transcription was insensitive to pertussis toxin, an inhibitor for G-proteins (Leaney and Tinker, 2000).

Thus, Ror2 alone is probably unable to induce PCKα translocation and both sFRP2 and Ror2 rather promote PKCα activation mediated through Fz7 receptors that are animally expressed in *Xenopus*. However, these findings do not provide sufficient information and it is difficult to say whether sFRP2 and Ror2 promote or just do not affect Fz7 induced PKCα membrane translocation. To obtain further evidence, it could be analyzed whether a knockdown of Fz7 prevents PCKα translocation observed in Ror2 over-expressing ACs and additionally test the effect of sFRP2 and Ror2 on other components of this signaling cascade.

In addition to PKCα, Fz7 can also trigger membrane translocation of PKCδ, which was demonstrated to be essential for Fz7 induced JNK activation and morphogenesis during *Xenopus* gastrulation (Kinoshita et al., 2003). There exist various members of the PKC family and each has a specific expression profile and is believed to play distinct roles. Similar to PKCα, PKCδ is sensitive to DAG, a substrate produced by Wnt/Ca^{2+} signaling (Toker, 1998). Focusing on the the localization PKCδ in *Xenopus* AC explants, sFRP2 as well as Ror2 reduced Fz7 mediated PKCδ recruitment (Fig. 24). Ror2 by itself was unable to recruit PKCδ to the membrane.

While canonical signaling is largely distinct from non-canonical Wnt signaling, single non-canonical Wnt branches partially overlap and can share several pathway components. The Wnt/PCP and Wnt/Ca^{2+} branches share common effectors and several reports suggest that they may be a joint part of a common non-canonical Wnt pathway. Notably, there is accumulating evidence that G-proteins play a role in all Wnt/Fz cascades. Fz receptors belong to the super family of G-protein coupled receptors and it was demonstrated that they interact with different types of heterotrimeric G-proteins (Katanaev et al., 2005; Koval and Katanaev, 2011; Nichols et al., 2013). However, it remains to be tested by loss of function experiments whether specific heterotrimeric G-proteins play a role in non-canonical Wnt signaling.

Collectively, the presented data show that sFRP2 and Ror2 inhibit the recruitment of PKCδ, in line with its known function in CE movements and Fz7 mediated JNK activation (Kinoshita et al., 2003). This is in agreement with the proposed hypothesis that sFRP2 and Ror2 antagonize Wnt/PCP signaling during CE.

In contrast, Fz7 mediated translocation of PCKα was not inhibited suggesting that they do not affect the process of tissue separation during *Xenopus* gastrulation. However, further studies are needed to prove this hypothesis.

4.4 sFRP2 and Ror2 prevent Fz7 receptor internalization and signaling

In the past, endocytosis has been considered mainly as a terminator of signaling by receptor turn-over but recent studies present evidence that Fz receptor internalization is a positive key player in many signaling events (Blitzer and Nusse, 2006; Kim et al., 2008; Ohkawara et al., 2011). In *Xenopus* dorsal marginal zone explants, a morpholino oligonucleotide mediated knockdown of Ror2 always resulted in a slightly higher Fz7 vesicle formation compared to those that only expressed Fz7-GFP (Fig. 26). Consistently, over-expression of Ror2 enhanced Fz7 accumulation at the membrane indicating that both proteins exert inhibitory effects on Fz7 endocytosis. However, in both experimental set ups, a stimulation with Wnt5a did not significantly increase Fz7 internalization which served as a positive control in this assay. It should be noted that Wnt proteins are highly expressed in the DMZ of a gastrulating *Xenopus* embryo and therefore the endogenous Wnt concentration might already be too high to induce stronger effect. Alternatively, it might be that injected Wnt proteins were not properly expressed in these experiments. Moreover, over-expressed Fz7-GFP was partially trapped in the ER and was not localized in clear patterns even at very low expression levels. It could be tested whether an mCherry or CFP tagged Fz7 version induces clearer results in these localization assays. Due to these technical problems, the localization of endogenous Fz7 in DMZ explants was further analyzed. Stimulation with Wnt5a enhanced the amount of intracellular Fz7 vesicles and consistent with previous observations, loss of sFRP2/Ror2 as well as a double knockdown reduced Fz7 membrane staining (Fig. 27). However, injected mbRFP RNA, which serves as a membrane marker, was not expressed in this experimental setup and therefore has to be reproduced. In addition, it has to be tested whether overexpression of sFRP2 or Ror2 enhance endogenous Fz7 membrane staining.

To verify the proposed hypothesis, I decided to include zebrafish as another vertebrate model system. In zebrafish, Wnt5a induced a clear formation of intracellular Fz7 vesicles (Fig. 28). This vesicle formation was strongly reduced when Ror2 is co-expressed demonstrating that Ror2 is able to retain Fz7 at the cell membrane. Moreover, Ror2 and Fz7 formed prominent clusters when Wnt5a was co-expressed indicating that Ror2/Fz7 cluster formation and complex stabilization

depends on the presence of Wnt. The Wnt5a-induced Ror2/Fz7 cluster formation is in line with previous findings that Wnt5a stimulates Ror2 clustering at the cell membrane in *Xenopus* tissues (Wallkamm et al., 2014) and Wnt5a enhances Fz7 binding to Ror2 (Nishita et al., 2010). However, it was shown that the CRD of Ror2 enhances Fz7 mediated clustering of Dvl2, which co-localizes with the Wnt/PCP effector Rac1 suggesting that Ror2 supports Fz7 triggered signaling (Nishita et al., 2010). At a first glance this is controversial to the inhibition of Fz7 specific signaling by Ror2 observed in our study. Still, it is not known yet whether the formation of Dvl2-Rac1 clusters alone is sufficient to activate signaling in mouse L-cells, or if these need to be internalized in complex with Fz7 to induce Wnt signaling. It remains to be shown whether Fz7 is also part of the observed Dvl2-Rac1complex or if Ror2, as in our study, traps Fz7 at the membrane and induces AP-1 via an alternative and Rac1 independent pathway, as shown for *Xenopus* (Schambony and Wedlich, 2007). Furthermore, the interaction of Fz7 and Ror2 could have different, context dependent effects in distinct cell lines and tissues. As an example, Ryk (atypical receptor related tyrosine kinase) was demonstrated to function as a co-receptor for Fz7 to promote Wnt11 mediated endocytosis of Dvl (Kim et al., 2008). Ryk is a one pass transmembrane protein with a Wnt inhibitory factor (WIF) motif unrelated to Fz-CRDs and maternally provided in *Xenopus*. Ror2, which is strongly up-regulated during gastrulation, might compete with Ryk in mesodermal tissue for Fz7 binding to antagonize their cooperating effect. Similar to this, the type of co-receptor expressed in a given tissue could determine whether Fz internalization and signaling is repressed or promoted. It would be interesting to test whether sFRPs have an impact on Ryk/Fz7 interaction.

In addition to Ror2, sFRP2 was also able to stabilize Fz7 at the cell membrane in *Xenopus* and zebrafish (Fig. 26, 27, 28) and a morpholino oligonucleotide mediated knockdown of sFRP2 slightly increased the amount of intracellular Fz7 vesicles in *Xenopus* dorsal marginal zone explants. However, sFRP2 did not induce such a strong Fz7 cluster formation as seen in Ror2 treated zebrafish animals, suggesting that the transmembrane and intracellular domain of Ror2 might serve as an anchor for Fz7. Analyses of the effect of a Ror2 mutant that lacks the C-terminal domain could give a hint whether the intracellular domain has an impact on Fz7 stabilization. Also, cell surface biotinylation and co-localization assays with effectors of the

endocytotic machinery would further support the hypothesis that Fz7 endocytosis and signaling is impeded in the presence sFRP2 and Ror2. The effect induced by sFRP2 is much weaker and the potential mechanism how it stabilizes Fz7 will be discussed below.

In summary, sFRP2 and Ror2 prevent Fz7 receptor endocytosis, which could provide a mechanism for the observed inhibition of Fz7 signal transduction.

The presented study demonstrates that the CRD motif in sFRPs interacts with different receptors and can act as a molecular switch to promote or repress specific β-catenin independent Wnt signaling branches. On the basis of these data, I propose following model: when each receptor is expressed alone and stimulated with Wnt5a, Ror2 signaling is mildly stimulated and the Fz7 receptor is internalized thereby activating the Fz7 signaling pathway (Fig. panel (A)). However, when sFRP2 is present in the extracellular space, it binds to Ror2 via its CRD and stabilizes Wnt5a/Ror2 complexes leading to a high Ror2 signaling activity. On the other hand, when sFRP2 binds to Fz7, this complex is stabilized at the cell membrane, preventing Fz7 endocytosis and thereby reducing Fz7 signaling (Fig. panel (B)). Independent of sFRP2, when both receptors are co-expressed they can directly interact and influence the signaling activity of the other, leading to enhanced Ror2 and reduced Fz7 signaling. The CRD of the corresponding receptor thereby substitutes the CRD of sFRP2 (Fig. panel (C)).

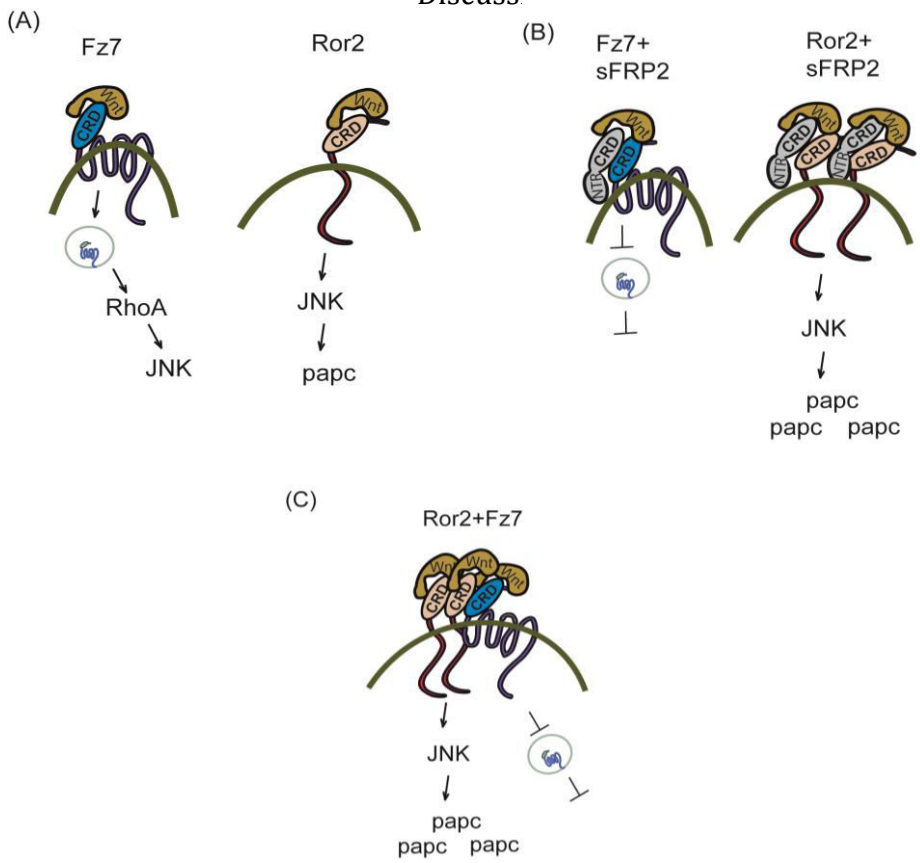

How can the divergent effects of sFRPs in different receptor contexts be explained? CRD-CRD interactions appear to be at the core of this regulatory mechanism. These data suggest that CRD heterodimers formed by the Ror2-CRD enhance signaling via this route whereas Fz7 heterodimers formed with Ror2 or sFRP-CRDs inhibit signaling and endocytosis of Fz7. On the other hand, forced Fz7 homodimerization has been shown to induce canonical Wnt signaling (Carron et al., 2003) . PCP signaling via Fz7 might therefore be generally inhibited by Wnt ligand binding to a Fz7 with dimeric CRD configuration, which probably precludes association with membrane-bound or cytoplasmic factors specific for the Fz-Rho signaling pathway (Habas et al., 2003). To solve this hypothesis, the role of the receptor-ligand stoichiometry in different non-canonical Wnt signaling cascades and the effect of sFRPs on the complex composition should be the focus of future studies.

4.5 Efficient Fz7 receptor inhibition requires both the CRD and NTR domain of sFRP2

At present, it is unclear how sFRP2 prevents Fz7 receptor endocytosis. The NTR domain of sFRP was suggested to interact with heparan proteoglycans and therefore might be responsible for sFRP association with the cell membrane (Finch et al., 1997). Indeed, sFRP2 lacking the NTR domain (sFRP2-CRD) was less potent in stabilizing Fz7 at the membrane (Fig. 29) indicating that the NTR domain of sFRP2 might be instrumental for efficient Fz7 receptor stabilization. Furthermore, preliminary data showed that sFRP2 lacking the NTR domain (sFRP2-CRD) could also not inhibit Fz7 mediated ATF activity. Interestingly, also the CRD deleted mutant did not inhibit but rather enhanced Fz7 signaling. These findings implicate that efficient inhibition of Fz7 receptor endocytosis and signaling by sFRP2 requires the presence of both the CRD and NTR domain.

The NTR domain of sFRP1 was demonstrated to interact with Wnt ligands and antagonizes their activity in the anterior neural plate (Lopez-Rios et al., 2008). It was shown that the CRD of sFRP1 binds to Fz5 whereas the NTR domain interacts with Wnt8. The NTR domain could mimic the function of the entire molecule and inhibit Wnt8 induced β-catenin signaling. This was also the case for the sFRP2-NTR mutant (Lopez-Rios et al., 2008; Uren et al., 2000). Interestingly, for sFRP3 the CRD was required and sufficient for the modulation of Wnt signaling. sFRP3 that lacks the CRD was unable to bind to Wnt1 and could not inhibit Wnt1 induced axis duplication (Lin et al., 1997). Sequence analysis revealed that the NTR motif of sFRP1, sFRP2 and sFRP5 share a similar cysteine pattern related to Netrin-1 whereas sFRP3 and sFRP4 display a different cysteine - spacing and a distinct pattern of disulphide bonds. Furthermore, sFRP1 is N-glycosylated and sulphated at two 2 tyrosine residues that are absent from sFRP2, -3 and - 4 (Chong et al., 2002; Zhong et al., 2007). Notably, plasmon-resonance binding studies demonstrated that Wnt3a, a ligand, which activates canonical Wnt signaling, binds at least two sites in sFRP1, 2 and sFRP4, and one in sFRP3. In contrast, Wnt5a which induces non-canonical Wnt signaling binds exclusively to sFRP1 and 2. The affinity of sFRPs to canonical Wnt ligands might be different to those of non-canonical Wnt ligands. It seems that there exist differences among sFRP family members how and which pathway they

prevalently interfere with. It will be of interest to study the effect of different sFRPs, their deletion constructs and chimeric constructs of their CRD and NTR domains on the Wnt5a/Ror2, Wnt/Fz7 and the other Wnt pathways.

In case of sFRP2 and with focus on non-canonical Wnt signaling, I assume that sFRP2-NTR binds and shuttles Wnt5a molecules to Fz7, which results in enhanced Fz7 signaling activity. Sequestered Wnt5a either has a higher affinity to the Fz7 receptor than to the NTR domain, or the NTR domain alone is unable to efficiently associate with both the Fz7/Wnt5a complex and membrane proteins. The Wnt5a/Fz7 complex is internalized alone or together with the NTR domain, which finally leads to signaling. The tertiary structure of sFRP2 therefore seems to be important to retain the Fz7/Wnt5a complex at the cell membrane. The CRD however can bind to Fz7 and is internalized together with Fz7 bound to Wn5a. This also mediated Fz7 signaling since it lacks the NTR domain which is essential to retain Fz7 at the cell membrane. In this context it would be interesting to examine whether the NTR of sFRP2 is also capable to interact with Fz7 and in addition to have a closer look on other sFRP family members, such as sFRP3 and sFRP4, and if they also have block Fz7 endocytosis and signaling.

5 Material and Methods

5.1 Materials

5.1.1 Antibodies

α-Digoxigenin-AP	sheep	Roche
α-flag, M2	mouse	Sigma
α-flag, OctAprobe	rabbit	Santa Cruz
α-V5	mouse	Invitrogen
α-myc, 9E10	mouse	Calbiochem
α-rabbit Alexa 488	goat	Invitrogen
α-mouse Alexa 488	goat	Molecular Probes
α-rabbit HRP	rabbit	Bio Rad
α-mouse HRP	goat	Bio Rad
α-mouse HA	mouse	Sigma
α-rabbit GFP	rabbit	Abcam

5.1.2 Buffer and Solutions

Cysteine solution	2% L-cysteine, pH 7.8
DMEM Ready mix	PAA, Sigma
DMEM High Glucose	PAA; Sigma
MBSH	88 mM Nacl, 1mm KCl, 2.4 mM NaHCO3, 0.33 mM Na(NO)3, 10 mM Hepes (pH 7.4)
MEMFA	100mM MOPS, 2 mM EGTA, 1mM $MgSO_4$, 3.7% Formaldehyde
MMR	100 mM NaCl, 2mM KCL,1 mM $MaSO_4$, 2 mM $CaCl_2$, 5 mM Hepes, pH 7.4
Mowiol	20 mg Mowiol, 50 ml Glycerol
PBS (10x)	137 mM NaCl, 27 mM KCl, 20 mm KH_2PO_4, 100 mM Na_2HPO_4 x $2H_2O$
PBST	1x PBS, 0.1% Tween-20
4% PFA/PBS	4% PFA in 1x PBS

pH 9 Buffer	0.1 M NaCl, 0.1 M Tris pH 9.5, 50 mm $MgCl_2$
3x SDS/Lämmli Buffer	150 mM Tris-HCl pH 6.8, 6% SDS, 0.3% Bromphenol blue, 30% Glycerol, 300 mM DTT
SDS-PAGE running Buffer	24.8 mM Tris, 192 mM glycine, 0.1 % SDS
SSC (20x)	3 m NaCl, 0.3 M sodium citrate, pH 7.5
Western Blot Transfer Buffer	10 mM Tris, 192 mM glycine, 20% methanol
TBE (10x)	89 mM Tris, 89 mM Boric acid, 2 mM EDTA
TBS (10x)	50 mM Tris-HCl, pH 7.4, 150 mM NaCl
Blocking solution (*In situ*)	2% BBR, 20% sheep serum in MABT
Blocking solution (Western Blot)	5% milk powder in 1x PBST
Blocking solution (IF)	3% BSA, 205 NGS, 0.1 M glycine in H_2O
Bleaching solution	15 H_2O_2, 5% formamide, 0.5 x SSC
BBR (10%)	10% Boehringer Blocking reagent, 1x MAB
BBR/MABT (2%)	1 v 10% BBR, 4 v MABT
Hybridization Buffer	5x SSC, 50% formamide, 1% BBR, 1 mg yeast tRNA, 0.1 mg heparin, 0.1 % Tween-20, 0.1 % Chaps, 5mM EDTA
LB medium	1% Bactotrypon,1% NaCl, 0.5% yeast extract
LB-Amp	1.5 % agarose, LB-medium, 50 mg/ml Ampicillin
MAB (10x)	1 M maleic acid, 1.5 M Nacl, pH 7.5
MABT	100mM Maleic acid, 150 mM NaCl, 0.1% Tween, pH 7.5
MEM (10x)	1M MOPS, 20 mM EGTA, 10 MM MgSO4 pH 7.4
NP40 Lysis Buffer	150 mM NaCl, 10 mM Tris/HCl, pH 7.8, 1 mM MgCl2, 0.75 mM CaCl2, 1% NP-40 and 0,3 mM OGP

5.1.3 Enzymes, Kits and Markers

BM Purple	Roche
Chorionic gonadotropin (human)	Sigma
Complete Mini Protease Inhibitor Cocktail Tablets	Roche
DIG-RNA labelling mix	Roche
EuroTaq DNA polymerase	Euroclone
FastDigest™ Resriction enzymes	Thermo Scientific
Page Rule™ Prestained Ladder	Thermo Scientific
GeneRuler™ 100bp and 1kb Ladder	Thermo Scientific
Proteinase K	Sigma
Phusion DNA Polymerase	Finnzymes
RT Maxima Reverse Transcriptase	Thermo Scientific
Midori Green Advanced or direct	Nippon Genetics
RNA Polymerase	Roche
T4 Polynucleotid kinase	
T4 DNA Ligase	Thermo Scientific
TurboFect™ Transfection reagent	Thermo Scientific
RiboLock RNAse inhibitor	Fermentas
DNase I	Fermentas
Turbo DNAse	Fermentas
Absolute QPCR SYBR® Green	Thermo Scientific
QIAquick Gel extraction kit	Qiagen
Super Signal West Femto Maximun Sensitivity Trail Kit	Thermo Scientific
Dual-Luciferase Reporter kit	Promega
mMessage mMachine High Capped RNA Transcrition kit (Sp6, T3, T7)	Ambion
Qiagen Plasmid Midi Kit	Qiagen

5.1.4 Oligonucleotides

qPCR

odc forward:	5'-GTCAATGATGGAGTGTATGGATC-3'
odc reverse:	5'-TCCATTCCGCTCTCCTGAGCAC-3'
xnr3 forward:	5´-CCAAAGCTTCATCGCTAA AAG-3´,
xnr3 reverse:	5´-AAAAGAAGGGAGGCAAATACG-3´
papc forward:	5'-CCCAGTCGGTCTCTTCTTCTTTG-3´
papc reverse:	5`-TTGCTGATGCTGCTCTTGGTTAG-3´
xbra forward:	5´-TTCAGCCTGTCTGTCAATGC-3 ´
xbra reverse:	5´-TGAGACACTGGTGTGATGGC-3´

Cloning:

CRD-HA forward:	5´-GCTCCTCTTCTAAGAAAACTCG-3´
CRD-HA reverse:	5'-CGATCTCCTTCACTTTTATCTTC-3'
NTR-HA forward:	5´-CGATCTCCTTCACTTTTATCTTC-3´
NTR-HA reverse:	5´- GCATCCGCAAGCTTCAG-3´

5.1.5 Antisense morpholino Oligonucleotides

All antisense morpholino oligonucleotides (Mos) used in this study were ordered from Gene Tool LLC. sFRP2 Mo (5´-AGCGCGACCCGCTGTGCCACATGAT -3´) covers the ATG region of x*sfrp2 (*BJ071409). All other Mo´s were previously described: Fz7 Mo (Winklbauer et al., 2001), Ror2 Mo and Standard Mo (Schambony and Wedlich, 2007), sFRP1 Mo2 (Gibb et al., 2013) and frzb2 (crescent) Mo (Shibata et al., 2005). All antisense Mos were injected with a concentration of 15 ng / embryo.

5.1.6 Plasmids

pCS2+NT7C5	(Swain et al., 2001)
pCS2+Fz7	(Medina and Steinbeisser, 2000)
pCS2+Fz7-myc	KM. Kürner
pCS2+Fz7-GFP	KM. Kürner
pCS2+PKCα- GFP	(Sheldahl et al., 1999)
pCS2+PKCδ- GFP	Amaya Manchester
pCS2+Ror2	(Hikasa et al., 2002)
pCS2+ Ror2 KD	(Hikasa et al., 2002)
pCS2+Wnt5a	(Moon et al., 1993)
pCS2+Wnt11	(Du et al., 1995)
pCS2+ Dkk3-HA	Andrey Glinka
pCS2+mouse Ror2-myc	Andrey Glinka
pCS2+mouse Ror2 ECD-flag	Andrey Glinka
pCS2+ mb-RFP	(Iioka et al., 2004)
pCMV-SPORT6+human sFRP2	(Invitrogen) (Ac.No: NM_003013)
pCS2+sFRP2-HA	Anne Gorny
pCS2+frzb2	Anne Gorny
M50-Super 8xTOP-Flash	(Biechele and Moon, 2008)
ATF2 reporter	(Ohkawara and Niehrs, 2011)

pCS2+sFRP2-CRD HA / pCS2+sFRP2-NTR-HA deletion constructs were generated from full length pCS2+sFRP2-HA by PCR amplification using the following primers: 5´-CGATCTCCTTCACTTTTATCTTC-3´and 5´- GCATCCGCAAGCTTCAG-3´ for pCS2+sFRP2-NTR HA and 5´-GCTCCTCTTCTAAGAAAACTCG-3´ and 5'-CGATCTCCTTCACTTTTATCTTC-3' for pCS2+sFRP2-CRD HA.
For zebrafish experiments all expression constructs were subcloned in pCS2+ (Rupp et al., 1994). cDNAs were obtained from xFz7, xRor2 and xWnt5a (Schambony and Wedlich, 2007). mem-mCherry, and GFP-GPI (Rengarajan et al., 2014).

5.1.7 Cells and Bacteria

E. coli XL1 (chemocompetent)

E. coli DH10B (electrocompetent)

Wnt5a-V5 producing mouse L-cells

Hek293 cells

5.1.8 Microscopes and Equipment

Axiophot stereomicroscope	Zeiss
DC350FX camera	Leica
C1 plus laser-scanning microscope	Nikon
TCS SP5 X confocal laser-scanning microscope	Leica
ND-1000 Spectrophotometer	NanoDrop
Lucy 2	Anthos Mikrosystems GmbH

5.1.9 Software

Image J

Photoshop

NIS-Elements Viewer 4.0, Nikon

Microsoft Excel

Imaris v7.5.2 software (Bitplane AG)

5.2 Nucleic acid methods

5.2.1 RNA Isolation

Total RNA from either 5 whole embryos at stage 11, 10 AC dissected at stage 8.5, or 10 DMZ explants dissected at stage 10.5 were cultivated until control embryos reached stage 12 and RNT was extracted using the MasterPure™ RNA Purification Kit (Epicenter Biotechnologies) according the manual instructions. The Quantity of total RNA was measured using a NanoDrop ND-1000 and RNA quality was checked by gel eletctrophoresis.

5.2.2 cDNA synthesis

To analyze the expression of the target gene by quantitative real time (qRT) PCR, extracted RNA (5.2.1) has to be reverse transcribed (RT-PCR) into cDNA. RNA was transcribed using random hexamer primers and reverse transcriptase RT Maxima (Fermentas). 500ng-1µg of total RNA was incubated in the following 20 µl reaction volume according to the program listed in Tab.1.

x µl	RNA
4 µl	5x RT buffer
1 µl	dNTPs
1 µl	Random Hexamer Primer
1 µl	RT Maxima
0.5 µl	Ribolock

The reaction volume was filled up to 20 µl with RNAse free water.

	Temperature	Time
	96 °C	2 min
25-30 x	94 °C 55-65 °C 72 °C	30 sec 30 sec 1 min
	72 °C	5 min
	4 °C	∞

Tab.1: PCR program used for RT-PCR

5.2.3 Quantitative real-time PCR

To quantify gene expression quantitative real PCR (qRT-PCR) was performed using SybrGreen Mix (Thermo Scientific) as a detection system. Reaction was carried out on a Real time PCR theromocycler (Analytik Jena) and set up in the following 10µl PCR reaction volume according to the program listed in Tab.2:

2 µl	cDNA sample
5 µl	SybrGreen Mix
0.4 µl	reverse primer
0.4 µl	forward primer
2.2 µl	water

	Temperature	Time
	95 °C	2 min
40x	95 °C	5 sec
	60 °C	15 sec
	melt	6 sec

Tab. 2: PCR program used for qRT-PCR

Expression levels were normalized to *ornithin-decarboxylase* (*odc*). Primer for *odc*: 5´-TGCACATGTCAAGCCAGTTC-3´, 5´-GCCCATC ACACGTTGGTC-3´; *xnr3*: 5´-CCAAAGCTTCATCGCTAA AAG-3´, 5´-AAAAGAAGGGAGGCAAATACG-3´; *papc*: 5'-CCCAGTCGGTCTCTTCTTCTTTG-3´, 5`-TTGCTGATGCTGCTCTTGGTTAG-3´. *xbra*: 5´-TTCAGCCTGTCTGTCAATGC-3 ´, 5´-TGAGACACTGGTGTGATGGC-3´.

5.2.4 DNA Isolation

For plasmid DNA isolation from bacteria (*E.coli* XL-1) the Midi-prep kit was used and performed according the manual. Single bacteria colonies were inoculated in LB-medium containing the corresponding antibiotic and incubated overnight at 37°C on a shaker. DNA isolation from agarose gels was performed using the QiaQuick DNA extraction kit according the manual instructions. To quantify the amount of isolated DNA, a spectrophotometer (NanoDrop) was used.

5.2.5 Restriction digests of plasmids

Restriction enzymes are prokaryotic endonucleases that recognize specific DNA sequences and can cut double stranded DNA at these sites. These enzymes either create a 5´- or 3´- overhang or blunt ends. Plasmids were digested using FastDigest restriction enzymes (Fermentas) according the manual. Reactions were incubated for 1 h at 37°C and the reaction was stopped either by heat inactivation or ethanol precipitation.

5.2.6 Nucleic acid precipitation

To precipitate nucleic acids, sample containing plasmid DNA is mixed with 1/10 volume of 3M natrium acetate and 3 volumes of 100% ethanol. After the sample was incubated for 30 min at -20°C, it is centrifuged at 13.000rpm for 15 min. The supernatant is removed and the pellet which contains the nucleic acids is washed once with 75% ethanol. After the pellet is air dried it is re-suspended in an appropriate volume of RNAse free water. Linearization and quality can be checked on an agarose gel (5.2.13) and is further serves as a template for Cap-RNA synthesis (5.2.7).

5.2.7 Cap RNA synthesis

For microinjections into *Xenopus* embryos, 5´-capped mRNAs have to be synthesized from linearized plasmids. A methylated guanine at the 5´-end is required for mRNA stability and attachment to the ribosome, where it is translated into a

protein. For this purpose the RNA Transcription kit (Ambion) was used and reaction was performed according the manual in the following 10µl reaction volume:

1 µg	linearized plasmid DNA
5 µl	2x NTP/CAP
1 µl	10 x reaction buffer
1 µl	Sp6/T7 or T3 enzyme mix
x µl	water

After the reaction was incubated for 3 h at 37°C, 1 µl Turbo DNAse was added and incubated for further 15 min to digest all residual DNA. To stop the reaction, 120 µl of water and 15 µl ammonium acetate stop solution were added to the sample and mixed vigorously. Synthesized Cap-RNA was then purified by phenol/chloroform (5.2.9).

5.2.8 DIG RNA synthesis

To detect endogenous RNA expressed in the *Xenopus* embryo, Digoxygenin (DIG) labeled antisense RNA was used. The labeling mix from Roche was used and RNA expression can be visualized by an enzymatic reaction. Linearized and purified DNA serves as a template for DIG RNA synthesis and the reaction was set up according the following equation:

1 µg	linearized plasmid
Add to 17 µl	water
2.5 µl	10x labeling mix
2.5 µl	10x polymerase buffer
0.5 µl	RNAse inhibitor
1.5 µl	RNA polymerase

Anti-sense probe against *papc* was synthesized from the pBS+PAPC full-length clone (Kim et al., 2000), linearized with XbaI and T7 RNA polymerase was used for *in vitro* transcription. The reaction was incubated for 3 h at 37°C and then precipitated by adding 1.5 µl 7.5M LiCl and 70 µl ice cold 100% ethanol. After this reaction was incubated for 30 min at -20°C, the sample was centrifuged at 13.000 rpm for 30 min at 4°C to pellet the DIG-RNA. The supernatant was removed and the pellet was washed twice with 75% ethanol and then air dried until DIG-RNA was re-supendend in 20µl 2x SSC/10% formamide. DIG-RNA can be stored at -20°C and quality is checked by gel electrophoresis (5.2.13).

5.2.9 RNA Purification by Phenol/Chloroform

Phenol/Chloroform extraction was used to separate Cap-RNA acids from proteins and lipids. In a first step, the nucleic acids solution is mixed with the same volume of Phenol-chloroform-isoamylalcohol. After the sample is centrifuged for 5 min at 12.000 rpm, the upper aqueous phase is transferred into a fresh tube. This solution is then mixed with an equal volume of chloroform-isoamylalcohol (1:24) and centrifuged for 5 min at 12.000 rpm. The upper phase is again transferred in a new tube and precipitated by isopropanol for minimum 30 min at -20°C. To pellet the nucleic acids, it is centrifuged at 12.000 rpm for 30 min. The supernatant is discarded and the pellet is washed once with 75% ethanol before it is re-suspended in an appropriate volume of water. The quality of purified Cap RNA can be checked on an agarose gel (5.2.13) and is ready to use for *Xenopus* microinjections (5.5.3). To quantify the amount of Cap-RNA, a spectrophotometer (NanoDrop) was used.

5.2.10 Polymerase chain reaction (PCR)

Temperature gradient PCR

For cloning purposes the proofreading Phusion DNA polymerase was used. To amplify single CRD and NTR domains of sFRP2 a temperature gradient PCR was performed using specific primers flanking the start site of each region (see 5.1.4). For both deletion construct, the following 50 µl reaction volume was used for amplification according to the PCR program in Tab 3.

1 ng	template plasmid
10 mM	dNTPs
1 µl	Primermix
10 µl	5x Phusion HF Buffer
0.5 µl	Pfu polymerase
x µl	water

For each deletion construct, seven reactions were set up and PCR was performed at the following temperatures:

57°C, 59°C, 60.2°C, 61.4°C, 62.6°C, 63.8°C, 65°C

	Temperature	Time
	98 °C	30 sec
	98 °C	10 sec
35x	see temp.	30 sec
	above	15 sec
	72 °C	10 sec

Tab.3: PCR program used for Cloning

Single amplified reactions were then separated on agarose gel (5.2.13). Specific bands were then cut out of the gel and purified using the QIAquick Gel extraction kit according the manual.

5.2.11 Phosphorylation and Ligation of amplified PCR products

Amplified PCR products were phosphorylated using a T4 Polynucleotid kinase and the reaction was set up as follows:

15 µl	template
2 µl	10x ReactionBuffer
2 µl	10 mM ATP
1 µl	T4 Polynucleotid kinase

This reaction was incubated for 20 min at 37°C and enzyme was heat inactivated for 10 min at 37°C. Phosphorylated blunt ends of amplified DNA segments were further ligated using a T4 Ligase in the following 20 µl reaction volume:

20-100 ng	phosphorylated plasmid
2 µl	10x Ligase Buffer
2 µl	50% PEG 4000 solution
1 µl	T4 Ligase
x µl	water

To check whether cloning was successful both generated constructs were double digested with specific restriction enzymes and analyzed by gel electrophoresis (5.2.13) and sequencing.

5.2.12 Chemical transformation in E.Coli

50 µl of chemocompetent *E. coli* XL1 cells were mixed with 100 µl of amplified plasmids and incubated for 20 min on ice. The plasmid cell suspension was heat shocked for 40 sec. at 42°C and then incubated for 2 min on ice. After transformation, bacteria were cultured in 800 µl LB-medium without antibiotics for 1 h at 37°C. 100 µl of this suspension was then plated on LB agar plates containing the corresponding antibiotic and incubated over night at 37°C.

5.2.13 Agarose Gel electrophoresis

Gel electrophoresis was used to analyze the quality of RNA or DNA fragments according their size. Agarose was melted in 1x TBE buffer and was polymerized in as gel-cast. For electrophoresis, the gel was placed in a chamber filled with 1xTBE buffer. DNA or RNA samples were mixed with 6x concentrated Midori Green direct (Nippon Genetics) and filled with water up to a total volume of 10µl. Samples were loaded into the single pockets of the agarose gel and nucleic acids were separated by electrophoresis under constant voltage. In addition, 6µl of a DNA protein ladder was used as a size standard. Nucleic acids were visualized by UV light exposure.

5.3 Cell culture methods

5.3.1 Cell culturing Hek293 and L-cells

Hek293 cells and Wnt5a-V5 producing L-cells were cultured in DMEM High Glucose containing 1% Penicillin/Streptavidin and 10% FCS in a 5% CO_2 incubator at 37°C. When cells were 80% confluent, they were treated with 1 ml Trypsin/EDTA for 1 min. When cells completely detached from the flask surface, 9 ml fresh culture medium was added. 1 ml of this cell suspension was then mixed with 15 ml culture medium in a fresh culture flask.

5.3.2 Transfection Hek293 cells

For transfection, cells were seeded in an appropriate density. 24h later they were transfected using TurboFect Transfection reagent. DNA, DMEM high Glucose without

serum and TurboFect reagent were mixed according the manual instructions. The solution was incubated for 20 min at RT and afterwards added dropwise to the cells. GFP was always used as a transfection control and to adapt protein amounts.

5.3.3 Conditioned media generation of L-cells

L-cells stably producing Wnt5a-V5 protein were seeded in an appropriate density in 10 cm petri dishes containing 15 ml culture medium. After 3 days of cultivation, complete supernatant was collected in a separate glass bottle. Fresh culture medium was added to the cells and incubated for further 3 days. Again, the supernatant was removed and mixed with the conditioned medium collected before. Conditioned media was filtered sterile using 0.2 µm Whatman filters, transferred in a fresh glass bottle and stored at 4°C for a maximum time of 2 month.

5.4 Biochemical and immunological methods

5.4.1 Immunoprecipitation

For immunoprecipitation experiments (IP) in Hek293 cells, 1µg of corresponding plasmids were transfected using Turbofect transfection reagent (Sigma). pCS2+mRor2-myc was transfected alone or together with either pCS2+sFRP2-HA or pCS2+sFRP2-NTR HA or pCS2+sFRP2-CRD HA. pCS2+GFP plasmid was used as a transfection control and to adapt transfected plasmid amounts. Hek293 cells were grown for 48 h in a 6-well culture dish. After cells were washed twice with 500 µl ice cold PBS, 400 µl NP40-Lysis buffer containing 10% protease-and phosphatase inhibitor was added to each well and incubated for 10 min at 4°C on a shaker. The cells were scraped off the well and cell solutions were then transferred into 1.5 ml tubes and further incubated for 40 min on an overhead-rotator. To pellet cell debris, tubes were centrifuged with 12.000 rpm for 20 min at 4 °C. After cells were lysed, the protein lysate was divided into three separate aliquots either incubated with a mouse anti-IgG antibody (Dianova), anti-myc antibody (1:100, Calbiochem) or a mouse anti-HA antibody (1:100, Sigma) to precipitate the corresponding tagged proteins. 50 µl was served as the input. 30 µl of magnetic bead suspension (Ademtech) were added to the immune complex and incubated for further 3 h at 4°C. Using a magnetic rack,

beads which bound to the immune complex were washed 3x with 500 µl Lysis buffer and were then re-suspended in 30 µl PAG elution buffer to elute the immune complex. The solution was mixed by pipetting up and down for 1 min. Beads were collected by a magnetic rack and supernatant, containing the immune complex was transferred to a new tube. For the binding assay in Hek293 cells, 1 µg of pCS2+mouseRor2 ECD flag was transfected alone or in combination with either pCS2+sFRP2-HA, pCS2+sFRP2-CRD HA, pCS2+Fz7- myc or pCS2+Dkk3-HA or pCS2+GFP. After 48 h of incubation, cells were washed with serum free media and were further incubated with Wnt5a-V5 conditioned media stably secreted by L-cells (Ohkawara et al., 2011) for 25 min. Cells were lysed in NP40 – Lysis buffer followed by the incubation with a rabbit anti-flag (OctAprobe: Santa Cruz). After the cell lysate was incubated for 2 h at 4°C on an overhead rotator, 50 µl magnetic bead suspension (Ademtech) was added and further incubated over night at 4 °C. After washing the precipitated proteins several times with ice-cold lysis buffer, lysates were re-suspended in PAG elution buffer (Adamtech).

Purified protein samples were mixed with 6x SDS-Laemmli buffer, heated up to 90 °C for 5 min and samples were then frozen at -80°C.

5.4.2 SDS-Page and Western Blot

Proteins were separated by SDS-polyacrylamide gel electrophoresis using a Novex XCell SureLock mini chamber. A 15% separating gel topped with a 4% stacking gel was prepared by polymerization as described (Laemmli 1970). 10µl of protein extracts were separated at constant voltage of 150V in SDS-PAGE running buffer. 6µl of a pre-stained protein ladder was used as a molecular weight standard. Afterwards, SDS-gel containing separated proteins were transferred on a nitrocellulose membrane by semi Dry western Blotting. After the protein transfer was checked by PonceauS staining the membrane was blocked in 5% milkpowder in PBST for 1 h at RT followed by incubation with the first antibody (see corresponding figure legends) over night at 4°C. Next day, membrane was washed 6x 15 min with PBST and further incubated for 1 h with secondary antibody at RT. For western blot analysis, a mouse anti-myc antibody (1:1000, Calbiochem), a mouse anti-V5 antibody (1:1000, Invitrogen), a mouse anti-flag antibody (1:1000, Sigma) or a mouse anti-HA antibody (1:1500, Sigma) were used.

Specific protein signals were visualized by the chemoluminscence SuperSignal west Femto Maximum Sensitivity Substrate trail Kit (Thermo Scientific) and further detected on X-ray film.

5.4.3 Renilla Luciferase Reporter Assay

For TopFlash Luciferase assay, 2-cell stage embryos were injected animally, into both blastomeres and for the ATF luciferase reporter assay, 4-cell stage embryos were injected into both animal ventral blastomeres. 100 pg of the ATF2-Luciferase-,or 80pg of the TopFlash reporter plasmid and 10 pg of the TK Renilla Luciferase reporter plasmid were either injected alone or together with indicated synthetic mRNAs in the figure legends. The ATF2 Luciferase reporter assays and TopFlash Luciferase assays were carried out from whole embryos lysed at gastrula stage 12 and stage 1, alternatively. Triplicates of 5-7 embryos each were homogenized on ice in 125 µl Passive Lysis buffer (Promega). To remove the cell debris, samples were centrifuged for 5 min once at 10000 rpm and then at 5000rpm. 20 µl of each embryo lysate without the fat layer was transferred in a 96 well plate and Luciferase activity was measured using the Dual luciferase system (Promega) according to manufacturer's instructions.

5.4.4 Immunostaining of *Xenopus* DMZ and AC explants

AC or DMZ explants of *Xenopus* embryos were fixed for 40 min at RT in 3.7% PFA/PBS. After explants were washed twice with PBS for 15 min, they were further incubated in Tris/NaCl for 30 min, followed by another 15 min in PBS. Explants were permeabilized in 0.3% Triton X-100/PBS for 10 min and then washed twice with PBS for 15 min before they were incubated in blocking solution for 1h at RT. Afterwards they were incubated with an anti-rabbit α-GFP antibody in blocking solution (1:10) overnight at 4°C. Explants were washed several times with PBS and were again incubated with a secondary α-rabbit Alexa 488 antibody (1:200) in blocking solution at 4°C overnight. After they were washed with PBS, explants were stained with Dapi/PBS and were finally mounted using Mowiol and a cover glass. Glass slides were dried over night at 4°C and then used for further analysis.

5.5 Embryological Methods

5.5.1 *Xenopus* egg collection

Xenopus laevis frogs were obtained from Nasco. All experiments complied with local and international guidelines for the use of experimental animals. Female Xenopus laevis frogs were injected with 400IU of human chorionic gonadotropin into the lymph sac. Around 10-12 hours after injection the frogs started to lay eggs. They were collected in a small petri dish and further used for *in vitro* fertilization.

5.5.2 *In vitro* fertilization

For preparation of the sperm solution, a piece of testis was cut off and homogenized in 500µl 1x MBSH. This solution was added on top of the eggs and were further spread out and arranged to a monolayer. They were covered with water which decreases the salt concentration and enables the sperm to move and fertilize the eggs. 40 minutes post fertalization they were de-jellied with 2% cysteine hydrochlorid, pH 7.8 by gentle agitation for not longer than 5 minutes. Fertilized embryos were washed 5x with water and twice with 1x MBSH. For experiments, embryos were microinjected in 1xMBSH and further cultured in 0.1× MBSH at 14-18°C.
Embryos were staged according to (Nieuwkoop and Faber, 1967) and dorsal blastomeres of 4 - cell embryos were identified according to (Klein, 1987).

5.5.3 Microinjection

In vitro synthesised 5´-capped RNA (5.2.7) or antisense morpholino oligonucleotides (5.1.5) were injected into *Xenopus* embryos by a IM300 Microinjector. The stage and side of injection depends on the single experiment and is mentioned in the corresponding figure legend. Embryos were placed in a small petris dish that is filled with 1x MBSH and covered with 1% agarose. Injection volume was calibrated to 5 nl. After injection, they were cultured for 1 h in 1x MBSH and then in 0.1 x MBSH. Injection sites, construct compositions and stages used in the individual experiments are indicated in the figure legends and in the following sections of Material and Methods.

5.5.4 Animal cap explants

For Animal Cap (AC) explants, embryos were injected animally into both blastomeres ACs can be explanted from blastula embryos at stage 9. By using fine forceps, the vitelline membrane is carefully removed without harming the embryo. In a next step, the embryo is oriented in such a way that the pigmented animal pole is faced up. The AC is then explanted and placed into a petri dish filled with 1x MBSH. ACs were either used for RNA extraction (5.2.1) or the AC elongation assay (5.5.5). ACs used to analyze the expression of *papc* or *xnr3*, were incubated for 5h at RT before RNA was extracted.

5.5.5 Animal cap elongation assay

For the elongation assay, ACs were dissected at stage 8.5 (5.5.4) and cultivated overnight in 0.5 x MBSH together with 10 ng/µl gentamycin and 50 ng/µl Activin on plates coated with BSA. For the analysis of *xbra* expression, AC explants were cultivated only for 2 h in Activin before total RNA was extracted for qPCR (5.2.1). When control embryos reached stage 26, the ACs were fixed in MEMFA (5.5.7) and scored for elongation. Elongated explants were classified into three subgroups: full elongation, partial elongation and no elongation.

5.5.6 Dorsal marginal zone explants

Embryos were injected into the dorsal equatorial zone at 4-cell and dorsal marginal zone (DMZ) explants were dissected from gastrula embryos at stage 10. After the vitelline membrane was removed, the dorsal third part of the embryo was removed as described (Shih and Keller, 1992). DMZ explants were placed in a petri dish filled with 1x MBSH and incubated for 2 h at RT before RNA was extracted (5.2.1).

5.5.7 Fixation of embryos

When embryos reached the desired stage, they were collected in a glass vial and fixed in 2 ml 1x MEMFA for 2h at RT or at 4°C overnight. Fixed embryos were washed twice with 1x PBS for 10 minutes and used directly for phenotypic analysis or *in situ* hybridization (5.5.8). For long-time storage they can be kept in 100% methanol at -20°C.

5.5.8 Whole mount *In situ* hybridization

Whole mount *in situ* hybridization is a technique used to visualize a spatial expression pattern of endogenous mRNA (Harland, 1991). For this method, an antisense RNA probe that is labeled with Digoxygenin coupled nucleotides (5.2.8) can hybridize to the endogenous target mRNA. This probe can be visualized by using an α-Digoxygenin labeled antibody coupled to alkaline phophatase which uses BM-purpel (Roche) as a substrate. For Whole-mount *in situ* hybridizations, 4-cell stage embryos were injected into the DMZ with morpholinos (5.1.5) and/or synthetic mRNAs (5.2.7). *In situ* hybridization was performed as follows:

Day 1:

- When embryos were kept in 100% Methanol, rehydrate them in 70%, 50% and 25% MeOH in PBST
- wash 2x 5 min in PBST
- Proteinase K digest: 10µg/ml in PBST, 20 min at RT
- wash 2x in PBST
- fixation in 3.7% PFA/PBS for 10 min at RT
- wash 4x 5 min in PBST
- 1 ml hybridization buffer 5 min at RT
- 1 ml pre-warmed hybridization buffer 1 h at 65 °C
- 1 ml fresh hybridization buffer 2-6h at 65°C
- Hybridization of antisense probes: 1µl probe/1 ml hybridization buffer

Day 2:

- Wash 1x 5 min with 50% formamid/ 0.1% Chaps/ 5x SSC(preheat to 65°C) at RT
- Wash 1x 5 min with 25% formamid/ 0.1% Chaps/ 3.5x SSC at RT
- Wash 1x 5 min with 50% formamid/ 0.1% Chaps (preheat to 37°C) at RT
- Wash 2x 25 min with 2x SSC /0.1% Chaps at 37°C
- Wash 1x 5 min with 0.2x SSC/0.1% Chaps at RT
- Wash 2x 30 min with 0.2x SSC/ 0.1 % Chaps at 60°C
- Wash 2x 10 min with 0.2x SSC/ 0.1% Chaps at RT
- Wash 1x 10 min with 0.2x SSC/ 0.1% Chaps: MABT (1.1) at RT
- Wash 2x 5 min and 2x10 min with MABT at RT
- Incubate embryos with 1ml MABT/ 2% Boehringer Blocking reagent (BBR)(Roche) for 1 h at RT
- Dilute α-Dig-AP antibody 1:10000 in MABT/ 2% BBR/ 20% heat inactivated sheep-serum albumin
- Incubate embryos in 1 ml α-Dig-AP solution at 4 °C overnight

Day 3:

- Wash 2x 20 min and 4x 1h with MABT at RT
- Wash 1x 15 min with pH 9 buffer at RT
- Mix BM Purpel with pH 9 buffer (1:1) and add 500µl to each vial
- Keep vials with embryos in the dark and check coloration under the microscope
- Wash 2x 5 min with 1x PBS at RT to stop colour reaction
- Fix embryos in 3.7% PFA/PBS over night at 4°C

Pigmented embryos were bleached using 1% H_2O_2/ 5% formamid in 0.5x SSC under intensive light.

5.6 Statistical Analysis

Significant levels of qPCR and ATF data were calculated using the One-way Anova analysis and the paired Student´s t-test (* $p \leq 0.05$; ** $p \leq 0.01$; *** $p \leq 0.001$). Calculations were performed using Microsoft Excel or SPSS.

6 Appendix

6.1 Index of Abbreviations

AC	animal cap
Amp	ampicillin
ATF2	activating transcription factor 2
BBR	boehringer blocking reagent
BSA	bovine serum albumin
cDNA	copy DNA
CE	convergent extension
dNTPs	nucleoside triphosphate
DNA	desoxyribonucleic acid
DMZ	dorsal marginal zone
Dvl	Dishevelled
E. coli	*Escherichia coli*
Fz7	Frizzled 7
GFP	Green fluorescent protein
GSK	glycogen synthase kinase
GTPase	GTPase activating proteins
hCG	human chorionic gonadotropin
HEPES	2-[4-(2-Hydroxyethyl)-1-piperazinyl]-ethansulfonic acid
Hek	human embryonic kidney
JNK	c-jun N-terminal kinase
ISH	whole mount *in situ* hybridization
MO	morpholino antisense oligonucleotide
mRNA	messenger ribonucleic acid
MEM	Modified Eagle´s Medium
PAPC	Paraxial Protocadherin
PCP	planar cell polarity
PCR	polymerase chain reaction
PKCα	protein kinase C alpha
Rac	Ras-related C3 botulinum toxin substrate

RhoA	Ras homolog gene family member A
rpm	rounds per minute
RFP	red fluorescent protein
RT	room temperature
SDS	sodium dodecyl sulfate polyacrylamide gel electrophoresis
st	stage
TEMED	N,N,N',N'-Tetramethylethylendiamin
Wnt	***W****ingless*; *I**nt***
wt	wild type
xbra	*Xenopus* brachyury

6.2 Index of figures

6.3 Index of tables

7 References

Afzal, A.R., and S. Jeffery. 2003. One gene, two phenotypes: ROR2 mutations in autosomal recessive Robinow syndrome and autosomal dominant brachydactyly type B. *Human mutation*. 22:1-11.

Afzal, A.R., A. Rajab, C.D. Fenske, M. Oldridge, N. Elanko, E. Ternes-Pereira, B. Tuysuz, V.A. Murday, M.A. Patton, A.O. Wilkie, and S. Jeffery. 2000. Recessive Robinow syndrome, allelic to dominant brachydactyly type B, is caused by mutation of ROR2. *Nature genetics*. 25:419-422.

Aguilera, O., M.F. Fraga, E. Ballestar, M.F. Paz, M. Herranz, J. Espada, J.M. Garcia, A. Munoz, M. Esteller, and J.M. Gonzalez-Sancho. 2006. Epigenetic inactivation of the Wnt antagonist DICKKOPF-1 (DKK-1) gene in human colorectal cancer. *Oncogene*. 25:4116-4121.

Akbarzadeh, S., L.M. Wheldon, S.M. Sweet, S. Talma, F.K. Mardakheh, and J.K. Heath. 2008. The deleted in brachydactyly B domain of ROR2 is required for receptor activation by recruitment of Src. *PloS one*. 3:e1873.

Axelrod, J.D., J.R. Miller, J.M. Shulman, R.T. Moon, and N. Perrimon. 1998. Differential recruitment of Dishevelled provides signaling specificity in the planar cell polarity and Wingless signaling pathways. *Genes & development*. 12:2610-2622.

Banyai, L., and L. Patthy. 1999. The NTR module: domains of netrins, secreted frizzled related proteins, and type I procollagen C-proteinase enhancer protein are homologous with tissue inhibitors of metalloproteases. *Protein science : a publication of the Protein Society*. 8:1636-1642.

Bhat, R.A., B. Stauffer, B.S. Komm, and P.V. Bodine. 2007. Structure-function analysis of secreted frizzled-related protein-1 for its Wnt antagonist function. *Journal of cellular biochemistry*. 102:1519-1528.

Biechele, T.L., and R.T. Moon. 2008. Assaying beta-catenin/TCF transcription with beta-catenin/TCF transcription-based reporter constructs. *Methods in molecular biology*. 468:99-110.

Blitzer, J.T., and R. Nusse. 2006. A critical role for endocytosis in Wnt signaling. *BMC cell biology*. 7:28.

Bovolenta, P., P. Esteve, J.M. Ruiz, E. Cisneros, and J. Lopez-Rios. 2008. Beyond Wnt inhibition: new functions of secreted Frizzled-related proteins in development and disease. *Journal of cell science*. 121:737-746.

Brieher, W.M., and B.M. Gumbiner. 1994. Regulation of C-cadherin function during activin induced morphogenesis of Xenopus animal caps. *The Journal of cell biology*. 126:519-527.

Cappuccio, I., A. Calderone, C.L. Busceti, F. Biagioni, F. Pontarelli, V. Bruno, M. Storto, G.T. Terstappen, G. Gaviraghi, F. Fornai, G. Battaglia, D. Melchiorri, R.S. Zukin, F. Nicoletti, and A. Caricasole. 2005. Induction of Dickkopf-1, a negative modulator of the Wnt pathway, is required for the development of ischemic neuronal death. *The Journal of neuroscience : the official journal of the Society for Neuroscience*. 25:2647-2657.

Caricasole, A., A. Copani, F. Caraci, E. Aronica, A.J. Rozemuller, A. Caruso, M. Storto, G. Gaviraghi, G.C. Terstappen, and F. Nicoletti. 2004. Induction of Dickkopf-1, a negative modulator of the Wnt pathway, is associated with neuronal degeneration in

Alzheimer's brain. *The Journal of neuroscience : the official journal of the Society for Neuroscience*. 24:6021-6027.

Carron, C., A. Pascal, A. Djiane, J.C. Boucaut, D.L. Shi, and M. Umbhauer. 2003. Frizzled receptor dimerization is sufficient to activate the Wnt/beta-catenin pathway. *Journal of cell science*. 116:2541-2550.

Chen, W., D. ten Berge, J. Brown, S. Ahn, L.A. Hu, W.E. Miller, M.G. Caron, L.S. Barak, R. Nusse, and R.J. Lefkowitz. 2003. Dishevelled 2 recruits beta-arrestin 2 to mediate Wnt5A-stimulated endocytosis of Frizzled 4. *Science*. 301:1391-1394.

Chong, J.M., A. Uren, J.S. Rubin, and D.W. Speicher. 2002. Disulfide bond assignments of secreted Frizzled-related protein-1 provide insights about Frizzled homology and netrin modules. *The Journal of biological chemistry*. 277:5134-5144.

Clevers, H., and R. Nusse. 2012. Wnt/beta-catenin signaling and disease. *Cell*. 149:1192-1205.

Cruciat, C.M., and C. Niehrs. 2013. Secreted and transmembrane wnt inhibitors and activators. *Cold Spring Harbor perspectives in biology*. 5:a015081.

De Langhe, E., C. Aznar-Lopez, V. De Vooght, J.A. Vanoirbeek, F.P. Luyten, and R.J. Lories. 2014. Secreted frizzled related proteins inhibit fibrosis in vitro but appear redundant in vivo. *Fibrogenesis & tissue repair*. 7:14.

Djiane, A., J. Riou, M. Umbhauer, J. Boucaut, and D. Shi. 2000. Role of frizzled 7 in the regulation of convergent extension movements during gastrulation in Xenopus laevis. *Development*. 127:3091-3100.

Du, S.J., S.M. Purcell, J.L. Christian, L.L. McGrew, and R.T. Moon. 1995. Identification of distinct classes and functional domains of Wnts through expression of wild-type and chimeric proteins in Xenopus embryos. *Molecular and cellular biology*. 15:2625-2634.

Edris, B., I. Espinosa, T. Muhlenberg, A. Mikels, C.H. Lee, S.E. Steigen, S. Zhu, K.D. Montgomery, A.J. Lazar, D. Lev, J.A. Fletcher, A.H. Beck, R.B. West, R. Nusse, and M. van de Rijn. 2012. ROR2 is a novel prognostic biomarker and a potential therapeutic target in leiomyosarcoma and gastrointestinal stromal tumour. *The Journal of pathology*. 227:223-233.

Fiedler, M., C. Mendoza-Topaz, T.J. Rutherford, J. Mieszczanek, and M. Bienz. 2011. Dishevelled interacts with the DIX domain polymerization interface of Axin to interfere with its function in down-regulating beta-catenin. *Proceedings of the National Academy of Sciences of the United States of America*. 108:1937-1942.

Finch, P.W., X. He, M.J. Kelley, A. Uren, R.P. Schaudies, N.C. Popescu, S. Rudikoff, S.A. Aaronson, H.E. Varmus, and J.S. Rubin. 1997. Purification and molecular cloning of a secreted, Frizzled-related antagonist of Wnt action. *Proceedings of the National Academy of Sciences of the United States of America*. 94:6770-6775.

Fujii, Y., T. Hoshino, and H. Kumon. 2014. Molecular simulation analysis of the structure complex of C2 domains of DKK family members and beta-propeller domains of LRP5/6: explaining why DKK3 does not bind to LRP5/6. *Acta medica Okayama*. 68:63-78.

Gibb, N., D.L. Lavery, and S. Hoppler. 2013. sfrp1 promotes cardiomyocyte differentiation in Xenopus via negative-feedback regulation of Wnt signalling. *Development*. 140:1537-1549.

Glickman, N.S., C.B. Kimmel, M.A. Jones, and R.J. Adams. 2003. Shaping the zebrafish notochord. *Development*. 130:873-887.

Gonzalez-Sancho, J.M., O. Aguilera, J.M. Garcia, N. Pendas-Franco, C. Pena, S. Cal, A. Garcia de Herreros, F. Bonilla, and A. Munoz. 2005. The Wnt antagonist

DICKKOPF-1 gene is a downstream target of beta-catenin/TCF and is downregulated in human colon cancer. *Oncogene*. 24:1098-1103.

Goodrich, L.V. 2008. The plane facts of PCP in the CNS. *Neuron*. 60:9-16.

Gordon, A., L. Southam, J. Loughlin, A.G. Wilson, I. Stockley, A.J. Hamer, R. Eastell, and J.M. Wilkinson. 2007. Variation in the secreted frizzled-related protein-3 gene and risk of osteolysis and heterotopic ossification after total hip arthroplasty. *Journal of orthopaedic research : official publication of the Orthopaedic Research Society*. 25:1665-1670.

Gorny, A.K., L.T. Kaufmann, R.K. Swain, and H. Steinbeisser. 2013. A secreted splice variant of the Xenopus frizzled-4 receptor is a biphasic modulator of Wnt signalling. *Cell communication and signaling : CCS*. 11:89.

Grumolato, L., G. Liu, P. Mong, R. Mudbhary, R. Biswas, R. Arroyave, S. Vijayakumar, A.N. Economides, and S.A. Aaronson. 2010. Canonical and noncanonical Wnts use a common mechanism to activate completely unrelated coreceptors. *Genes & development*. 24:2517-2530.

Habas, R., I.B. Dawid, and X. He. 2003. Coactivation of Rac and Rho by Wnt/Frizzled signaling is required for vertebrate gastrulation. *Genes & development*. 17:295-309.

Hagemann, A.I., J. Kurz, S. Kauffeld, Q. Chen, P.M. Reeves, S. Weber, S. Schindler, G. Davidson, T. Kirchhausen, and S. Scholpp. 2014. In vivo analysis of formation and endocytosis of the Wnt/beta-catenin signaling complex in zebrafish embryos. *Journal of cell science*. 127:3970-3982.

Harland, R.M. 1991. In situ hybridization: an improved whole-mount method for Xenopus embryos. *Methods in cell biology*. 36:685-695.

Hikasa, H., M. Shibata, I. Hiratani, and M. Taira. 2002. The Xenopus receptor tyrosine kinase Xror2 modulates morphogenetic movements of the axial mesoderm and neuroectoderm via Wnt signaling. *Development*. 129:5227-5239.

Ho, H.Y., M.W. Susman, J.B. Bikoff, Y.K. Ryu, A.M. Jonas, L. Hu, R. Kuruvilla, and M.E. Greenberg. 2012. Wnt5a-Ror-Dishevelled signaling constitutes a core developmental pathway that controls tissue morphogenesis. *Proceedings of the National Academy of Sciences of the United States of America*. 109:4044-4051.

Iioka, H., N. Ueno, and N. Kinoshita. 2004. Essential role of MARCKS in cortical actin dynamics during gastrulation movements. *The Journal of cell biology*. 164:169-174.

Isaacs, H.V., M.E. Pownall, and J.M. Slack. 1994. eFGF regulates Xbra expression during Xenopus gastrulation. *The EMBO journal*. 13:4469-4481.

Itoh, K., J. Jacob, and Y.S. S. 1998. A role for Xenopus Frizzled 8 in dorsal development. *Mechanisms of development*. 74:145-157.

Katanaev, V.L., R. Ponzielli, M. Semeriva, and A. Tomlinson. 2005. Trimeric G protein-dependent frizzled signaling in Drosophila. *Cell*. 120:111-122.

Kawano, Y., and R. Kypta. 2003. Secreted antagonists of the Wnt signalling pathway. *Journal of cell science*. 116:2627-2634.

Keller, R. 2002. Shaping the vertebrate body plan by polarized embryonic cell movements. *Science*. 298:1950-1954.

Keller, R.E. 1980. The cellular basis of epiboly: an SEM study of deep-cell rearrangement during gastrulation in Xenopus laevis. *Journal of embryology and experimental morphology*. 60:201-234.

Keller, R.E. 1981. An experimental analysis of the role of bottle cells and the deep marginal zone in gastrulation of Xenopus laevis. *The Journal of experimental zoology*. 216:81-101.

Keller, R.E., M. Danilchik, R. Gimlich, and J. Shih. 1985. The function and mechanism of convergent extension during gastrulation of Xenopus laevis. *Journal of embryology and experimental morphology*. 89 Suppl:185-209.

Kikuchi, A., H. Yamamoto, A. Sato, and S. Matsumoto. 2011. New insights into the mechanism of Wnt signaling pathway activation. *International review of cell and molecular biology*. 291:21-71.

Kim, G.H., J.H. Her, and J.K. Han. 2008. Ryk cooperates with Frizzled 7 to promote Wnt11-mediated endocytosis and is essential for Xenopus laevis convergent extension movements. *The Journal of cell biology*. 182:1073-1082.

Kim, S.H., W.C. Jen, E.M. De Robertis, and C. Kintner. 2000. The protocadherin PAPC establishes segmental boundaries during somitogenesis in xenopus embryos. *Current biology : CB*. 10:821-830.

Kinoshita, N., H. Iioka, A. Miyakoshi, and N. Ueno. 2003. PKC delta is essential for Dishevelled function in a noncanonical Wnt pathway that regulates Xenopus convergent extension movements. *Genes & development*. 17:1663-1676.

Klein, S.L. 1987. The first cleavage furrow demarcates the dorsal-ventral axis in Xenopus embryos. *Developmental biology*. 120:299-304.

Komiya, Y., and R. Habas. 2008. Wnt signal transduction pathways. *Organogenesis*. 4:68-75.

Koval, A., and V.L. Katanaev. 2011. Wnt3a stimulation elicits G-protein-coupled receptor properties of mammalian Frizzled proteins. *The Biochemical journal*. 433:435-440.

Kuhl, M., K. Geis, L.C. Sheldahl, T. Pukrop, R.T. Moon, and D. Wedlich. 2001. Antagonistic regulation of convergent extension movements in Xenopus by Wnt/beta-catenin and Wnt/Ca2+ signaling. *Mechanisms of development*. 106:61-76.

Kuhl, M., L.C. Sheldahl, C.C. Malbon, and R.T. Moon. 2000a. Ca(2+)/calmodulin-dependent protein kinase II is stimulated by Wnt and Frizzled homologs and promotes ventral cell fates in Xenopus. *The Journal of biological chemistry*. 275:12701-12711.

Kuhl, M., L.C. Sheldahl, M. Park, J.R. Miller, and R.T. Moon. 2000b. The Wnt/Ca2+ pathway: a new vertebrate Wnt signaling pathway takes shape. *Trends in genetics : TIG*. 16:279-283.

Kumar, S., M. Zigman, T.R. Patel, B. Trageser, J.C. Gross, K. Rahm, M. Boutros, D. Gradl, H. Steinbeisser, T. Holstein, J. Stetefeld, and S. Ozbek. 2014. Molecular dissection of Wnt3a-Frizzled8 interaction reveals essential and modulatory determinants of Wnt signaling activity. *BMC biology*. 12:44.

Leaney, J.L., and A. Tinker. 2000. The role of members of the pertussis toxin-sensitive family of G proteins in coupling receptors to the activation of the G protein-gated inwardly rectifying potassium channel. *Proceedings of the National Academy of Sciences of the United States of America*. 97:5651-5656.

Lee, J.Y., and R.M. Harland. 2010. Endocytosis is required for efficient apical constriction during Xenopus gastrulation. *Current biology : CB*. 20:253-258.

Leyns, L., T. Bouwmeester, S.H. Kim, S. Piccolo, and E.M. De Robertis. 1997. Frzb-1 is a secreted antagonist of Wnt signaling expressed in the Spemann organizer. *Cell*. 88:747-756.

Li, Y., S.A. Rankin, D. Sinner, A.P. Kenny, P.A. Krieg, and A.M. Zorn. 2008. Sfrp5 coordinates foregut specification and morphogenesis by antagonizing both canonical and noncanonical Wnt11 signaling. *Genes & development*. 22:3050-3063.

Lin, K., S. Wang, M.A. Julius, J. Kitajewski, M. Moos, Jr., and F.P. Luyten. 1997. The cysteine-rich frizzled domain of Frzb-1 is required and sufficient for modulation of Wnt signaling. *Proceedings of the National Academy of Sciences of the United States of America*. 94:11196-11200.

Liu, Y., J.F. Ross, P.V. Bodine, and J. Billiard. 2007. Homodimerization of Ror2 tyrosine kinase receptor induces 14-3-3(beta) phosphorylation and promotes osteoblast differentiation and bone formation. *Molecular endocrinology*. 21:3050-3061.

Liu, Y., B. Rubin, P.V. Bodine, and J. Billiard. 2008. Wnt5a induces homodimerization and activation of Ror2 receptor tyrosine kinase. *Journal of cellular biochemistry*. 105:497-502.

Lopez-Rios, J., P. Esteve, J.M. Ruiz, and P. Bovolenta. 2008. The Netrin-related domain of Sfrp1 interacts with Wnt ligands and antagonizes their activity in the anterior neural plate. *Neural development*. 3:19.

Mao, B., and C. Niehrs. 2003. Kremen2 modulates Dickkopf2 activity during Wnt/LRP6 signaling. *Gene*. 302:179-183.

Masiakowski, P., and R.D. Carroll. 1992. A novel family of cell surface receptors with tyrosine kinase-like domain. *The Journal of biological chemistry*. 267:26181-26190.

McCrea, P.D., W.M. Brieher, and B.M. Gumbiner. 1993. Induction of a secondary body axis in Xenopus by antibodies to beta-catenin. *The Journal of cell biology*. 123:477-484.

Medina, A., W. Reintsch, and H. Steinbeisser. 2000. Xenopus frizzled 7 can act in canonical and non-canonical Wnt signaling pathways: implications on early patterning and morphogenesis. *Mechanisms of development*. 92:227-237.

Medina, A., and H. Steinbeisser. 2000. Interaction of Frizzled 7 and Dishevelled in Xenopus. *Developmental dynamics : an official publication of the American Association of Anatomists*. 218:671-680.

Mellor, H., and P.J. Parker. 1998. The extended protein kinase C superfamily. *The Biochemical journal*. 332 (Pt 2):281-292.

Mii, Y., and M. Taira. 2009. Secreted Frizzled-related proteins enhance the diffusion of Wnt ligands and expand their signalling range. *Development*. 136:4083-4088.

Mikels, A., Y. Minami, and R. Nusse. 2009. Ror2 receptor requires tyrosine kinase activity to mediate Wnt5A signaling. *The Journal of biological chemistry*. 284:30167-30176.

Moon, R.T., R.M. Campbell, J.L. Christian, L.L. McGrew, J. Shih, and S. Fraser. 1993. Xwnt-5A: a maternal Wnt that affects morphogenetic movements after overexpression in embryos of Xenopus laevis. *Development*. 119:97-111.

Munro, E.M., and G. Odell. 2002. Morphogenetic pattern formation during ascidian notochord formation is regulative and highly robust. *Development*. 129:1-12.

Myers, D.C., D.S. Sepich, and L. Solnica-Krezel. 2002. Bmp activity gradient regulates convergent extension during zebrafish gastrulation. *Developmental biology*. 243:81-98.

Nichols, A.S., D.H. Floyd, S.P. Bruinsma, K. Narzinski, and T.J. Baranski. 2013. Frizzled receptors signal through G proteins. *Cellular signalling*. 25:1468-1475.

Niehrs, C. 2006. Function and biological roles of the Dickkopf family of Wnt modulators. *Oncogene*. 25:7469-7481.

Niehrs, C. 2012. The complex world of WNT receptor signalling. *Nature reviews. Molecular cell biology*. 13:767-779.

Nishita, M., S. Itsukushima, A. Nomachi, M. Endo, Z. Wang, D. Inaba, S. Qiao, S. Takada, A. Kikuchi, and Y. Minami. 2010. Ror2/Frizzled complex mediates Wnt5a-induced AP-1 activation by regulating Dishevelled polymerization. *Molecular and cellular biology*. 30:3610-3619.

Nubler-Jung, K., R. Bonitz, and M. Sonnenschein. 1987. Cell polarity during wound healing in an insect epidermis. *Development*. 100:163-170.

Ohkawara, B., A. Glinka, and C. Niehrs. 2011. Rspo3 binds syndecan 4 and induces Wnt/PCP signaling via clathrin-mediated endocytosis to promote morphogenesis. *Developmental cell*. 20:303-314.

Ohkawara, B., and C. Niehrs. 2011. An ATF2-based luciferase reporter to monitor non-canonical Wnt signaling in Xenopus embryos. *Developmental dynamics : an official publication of the American Association of Anatomists*. 240:188-194.

Oldridge, M., A.M. Fortuna, M. Maringa, P. Propping, S. Mansour, C. Pollitt, T.M. DeChiara, R.B. Kimble, D.M. Valenzuela, G.D. Yancopoulos, and A.O. Wilkie. 2000. Dominant mutations in ROR2, encoding an orphan receptor tyrosine kinase, cause brachydactyly type B. *Nature genetics*. 24:275-278.

Pera, E.M., and E.M. De Robertis. 2000. A direct screen for secreted proteins in Xenopus embryos identifies distinct activities for the Wnt antagonists Crescent and Frzb-1. *Mechanisms of development*. 96:183-195.

Pinho, S., and C. Niehrs. 2007. Dkk3 is required for TGF-beta signaling during Xenopus mesoderm induction. *Differentiation; research in biological diversity*. 75:957-967.

Rengarajan, C., A. Matzke, L. Reiner, V. Orian-Rousseau, and S. Scholpp. 2014. Endocytosis of Fgf8 is a double-stage process and regulates spreading and signaling. *PloS one*. 9:e86373.

Rubin, J.S., M. Barshishat-Kupper, F. Feroze-Merzoug, and Z.F. Xi. 2006. Secreted WNT antagonists as tumor suppressors: pro and con. *Frontiers in bioscience : a journal and virtual library*. 11:2093-2105.

Rupp, R.A., L. Snider, and H. Weintraub. 1994. Xenopus embryos regulate the nuclear localization of XMyoD. *Genes & development*. 8:1311-1323.

Saldanha, J., J. Singh, and D. Mahadevan. 1998. Identification of a Frizzled-like cysteine rich domain in the extracellular region of developmental receptor tyrosine kinases. *Protein science : a publication of the Protein Society*. 7:1632-1635.

Satoh, W., T. Gotoh, Y. Tsunematsu, S. Aizawa, and A. Shimono. 2006. Sfrp1 and Sfrp2 regulate anteroposterior axis elongation and somite segmentation during mouse embryogenesis. *Development*. 133:989-999.

Satoh, W., M. Matsuyama, H. Takemura, S. Aizawa, and A. Shimono. 2008. Sfrp1, Sfrp2, and Sfrp5 regulate the Wnt/beta-catenin and the planar cell polarity pathways during early trunk formation in mouse. *Genesis*. 46:92-103.

Sausedo, R.A., and G.C. Schoenwolf. 1994. Quantitative analyses of cell behaviors underlying notochord formation and extension in mouse embryos. *The Anatomical record*. 239:103-112.

Schambony, A., and D. Wedlich. 2007. Wnt-5A/Ror2 regulate expression of XPAPC through an alternative noncanonical signaling pathway. *Developmental cell*. 12:779-792.

Schoenwolf, G.C., and I.S. Alvarez. 1989. Roles of neuroepithelial cell rearrangement and division in shaping of the avian neural plate. *Development*. 106:427-439.

Schwarz-Romond, T., M. Fiedler, N. Shibata, P.J. Butler, A. Kikuchi, Y. Higuchi, and M. Bienz. 2007. The DIX domain of Dishevelled confers Wnt signaling by dynamic polymerization. *Nature structural & molecular biology*. 14:484-492.

Seitz, K., V. Dursch, J. Harnos, V. Bryja, M. Gentzel, and A. Schambony. 2014. beta-Arrestin interacts with the beta/gamma subunits of trimeric G-proteins and dishevelled in the Wnt/Ca(2+) pathway in xenopus gastrulation. *PloS one*. 9:e87132.

Sheldahl, L.C., M. Park, C.C. Malbon, and R.T. Moon. 1999. Protein kinase C is differentially stimulated by Wnt and Frizzled homologs in a G-protein-dependent manner. *Current biology : CB*. 9:695-698.

Shibata, M., M. Itoh, H. Hikasa, S. Taira, and M. Taira. 2005. Role of crescent in convergent extension movements by modulating Wnt signaling in early Xenopus embryogenesis. *Mechanisms of development*. 122:1322-1339.

Shih, J., and R. Keller. 1992. The epithelium of the dorsal marginal zone of Xenopus has organizer properties. *Development*. 116:887-899.

Simons, M., and M. Mlodzik. 2008. Planar cell polarity signaling: from fly development to human disease. *Annual review of genetics*. 42:517-540.

Skah, S., J. Nadjar, M. Sirakov, and M. Plateroti. 2015. The secreted Frizzled-Related Protein 2 modulates cell fate and the Wnt pathway in the murine intestinal epithelium. *Experimental cell research*. 330:56-65.

Stanganello, E., A.I. Hagemann, B. Mattes, C. Sinner, D. Meyen, S. Weber, A. Schug, E. Raz, and S. Scholpp. 2015. Filopodia-based Wnt transport during vertebrate tissue patterning. *Nature communications*. 6:5846.

Sugiyama, Y., R.J. Stump, A. Nguyen, L. Wen, Y. Chen, Y. Wang, J.N. Murdoch, F.J. Lovicu, and J.W. McAvoy. 2010. Secreted frizzled-related protein disrupts PCP in eye lens fiber cells that have polarised primary cilia. *Developmental biology*. 338:193-201.

Sumanas, S., and S.C. Ekker. 2001. Xenopus frizzled-7 morphant displays defects in dorsoventral patterning and convergent extension movements during gastrulation. *Genesis*. 30:119-122.

Swain, R.K., A. Medina, and H. Steinbeisser. 2001. Functional analysis of the Xenopus frizzled 7 protein domains using chimeric receptors. *The International journal of developmental biology*. 45:259-264.

Tauriello, D.V., I. Jordens, K. Kirchner, J.W. Slootstra, T. Kruitwagen, B.A. Bouwman, M. Noutsou, S.G. Rudiger, K. Schwamborn, A. Schambony, and M.M. Maurice. 2012. Wnt/beta-catenin signaling requires interaction of the Dishevelled DEP domain and C terminus with a discontinuous motif in Frizzled. *Proceedings of the National Academy of Sciences of the United States of America*. 109:E812-820.

To, K.F., M.W. Chan, W.K. Leung, J. Yu, J.H. Tong, T.L. Lee, F.K. Chan, and J.J. Sung. 2001. Alterations of frizzled (FzE3) and secreted frizzled related protein (hsFRP) expression in gastric cancer. *Life sciences*. 70:483-489.

Toker, A. 1998. Signaling through protein kinase C. *Frontiers in bioscience : a journal and virtual library*. 3:D1134-1147.

Torres, M.A., J.A. Yang-Snyder, S.M. Purcell, A.A. DeMarais, L.L. McGrew, and R.T. Moon. 1996. Activities of the Wnt-1 class of secreted signaling factors are antagonized by the Wnt-5A class and by a dominant negative cadherin in early Xenopus development. *The Journal of cell biology*. 133:1123-1137.

Turashvili, G., J. Bouchal, G. Burkadze, and Z. Kolar. 2006. Wnt signaling pathway in mammary gland development and carcinogenesis. *Pathobiology : journal of immunopathology, molecular and cellular biology*. 73:213-223.

Uren, A., F. Reichsman, V. Anest, W.G. Taylor, K. Muraiso, D.P. Bottaro, S. Cumberledge, and J.S. Rubin. 2000. Secreted frizzled-related protein-1 binds directly to Wingless and is a biphasic modulator of Wnt signaling. *The Journal of biological chemistry*. 275:4374-4382.

Veeman, M.T., D.C. Slusarski, A. Kaykas, S.H. Louie, and R.T. Moon. 2003. Zebrafish prickle, a modulator of noncanonical Wnt/Fz signaling, regulates gastrulation movements. *Current biology : CB*. 13:680-685.

Wallingford, J.B., S.E. Fraser, and R.M. Harland. 2002. Convergent extension: the molecular control of polarized cell movement during embryonic development. *Developmental cell*. 2:695-706.

Wallkamm, V., R. Dorlich, K. Rahm, T. Klessing, G.U. Nienhaus, D. Wedlich, and D. Gradl. 2014. Live imaging of Xwnt5A-ROR2 complexes. *PloS one*. 9:e109428.

Wang, Y., and H. Steinbeisser. 2009. Molecular basis of morphogenesis during vertebrate gastrulation. *Cellular and molecular life sciences : CMLS*. 66:2263-2273.

Wawrzak, D., M. Metioui, E. Willems, M. Hendrickx, E. de Genst, and L. Leyns. 2007. Wnt3a binds to several sFRPs in the nanomolar range. *Biochemical and biophysical research communications*. 357:1119-1123.

Winklbauer, R., A. Medina, R.K. Swain, and H. Steinbeisser. 2001. Frizzled-7 signalling controls tissue separation during Xenopus gastrulation. *Nature*. 413:856-860.

Yamamoto, H., S.K. Yoo, M. Nishita, A. Kikuchi, and Y. Minami. 2007. Wnt5a modulates glycogen synthase kinase 3 to induce phosphorylation of receptor tyrosine kinase Ror2. *Genes to cells : devoted to molecular & cellular mechanisms*. 12:1215-1223.

Yu, A., Y. Xing, S.C. Harrison, and T. Kirchhausen. 2010. Structural analysis of the interaction between Dishevelled2 and clathrin AP-2 adaptor, a critical step in noncanonical Wnt signaling. *Structure*. 18:1311-1320.

Yuan, Y., C.C. Niu, G. Deng, Z.Q. Li, J. Pan, C. Zhao, Z.L. Yang, and W.K. Si. 2011. The Wnt5a/Ror2 noncanonical signaling pathway inhibits canonical Wnt signaling in K562 cells. *International journal of molecular medicine*. 27:63-69.

Zhong, X., T. Desilva, L. Lin, P. Bodine, R.A. Bhat, E. Presman, J. Pocas, M. Stahl, and R. Kriz. 2007. Regulation of secreted Frizzled-related protein-1 by heparin. *The Journal of biological chemistry*. 282:20523-20533.

Zi, X., Y. Guo, A.R. Simoneau, C. Hope, J. Xie, R.F. Holcombe, and B.H. Hoang. 2005. Expression of Frzb/secreted Frizzled-related protein 3, a secreted Wnt antagonist, in human androgen-independent prostate cancer PC-3 cells suppresses tumor growth and cellular invasiveness. *Cancer research*. 65:9762-9770.